A Reassessment of Trajectory Options for Human Missions to Mars

Damon F. Landau* and James M. Longuski†
Purdue University, West Lafayette, IN, 47907-2023

Earth-Mars trajectories with low-energy requirements that also limit the (transfer) time a crew spends in interplanetary space are essential to the design of cost-effective, minimal-risk missions. We compute optimal ΔV trajectories with constraints on the transfer time of flight (TOF) for launch years 2009 through 2022. We further explore the consequences of specifying different TOF limits (from 120 to 270 days) for human missions to Mars. In addition to direct trajectories, we also calculate optimal free-return, Mars-Earth semi-cycler, Earth-Mars semi-cycler, and cycler trajectories. The trades between powered and aero-assisted planetary capture for each trajectory type are also examined. We find that as the number of flybys increase (i.e. free-returns have one flyby, semi-cyclers may have from two to four flybys, and cyclers have an unlimited number of flybys), the V_∞ generally increase, but the mission mass decreases because smaller vehicles may be used. We also compute optimal low-thrust transfers (with constant thrust and constant I_{sp}) between Earth and Mars over a range of TOF, and note that the optimal ΔV for a specified burn-time and TOF is nearly constant. This property provides a means to quickly establish mass and thrust requirements to achieve a desired TOF for any vehicle mass and specific impulse. As expected, the energy requirements of the trajectories decrease with increasing TOF, and the optimal ΔV is reduced by up to 50% when the TOF limit is increased from the NASA-recommended 180 days to 270 days. Our results are compiled into sets of plots that describe the optimal, constrained TOF trajectories for use in Mars mission studies.

Nomenclature

a	=	acceleration, m/s^2
g	=	standard acceleration due to gravity at Earth's surface, 9.80665 m/s^2
I_{sp}	=	specific impulse, s
m_0	=	initial mass, mt
m_f	=	final mass, mt
$\dot{m}$	=	mass flow rate, kg/s
T	=	thrust, N
t_b	=	burn time, s

I. Introduction

With the advent of the space age, the long-standing aspiration of sending explorers to Mars is becoming a reality. Indeed, there have been many investigations into the best way to conduct human missions to Mars.[1-16] Typical mission scenarios are either short duration (about 600 days with 30-day Mars stay time) or long stay time (about 550 days with 900-day mission duration). Opposition class trajectories[17-26] provide direct transfers for short duration missions, while conjunction class trajectories[22-33] are applicable to long stay time missions. In addition to these direct transfers, a mission to Mars could incorporate free-return trajectories,[34-41] Mars-Earth semi-cyclers,[42,43] Earth-Mars semi-cyclers, or cyclers.[44-49]

* Graduate Student, School of Aeronautics and Astronautics, 315 N. Grant St., Student Member AIAA.
† Professor, School of Aeronautics and Astronautics, 315 N. Grant St., Associate Fellow AIAA.

Two key issues with human spaceflight are the deleterious effects of zero-gravity and radiation. Consequently, the time of flight (TOF) between Earth and Mars is often constrained to reduce the time the crew must spend in interplanetary space. To examine the effects of limiting TOF, we compute optimal ΔV trajectories (to reduce mission cost) with constrained TOF (to reduce mission risk). We consider a range of TOF from 120 days to 270 days. Unfortunately, trajectories between Earth and Mars with short TOF, short mission duration, *and* low energy requirements (low ΔV) do not exist; thus, we do not include opposition class trajectories in our analysis. Instead, we examine impulsive ΔV direct, free-return, semi-cycler, and cycler trajectories as well as direct low-thrust[50-60] (with constant thrust and constant I_{sp}) missions. The effects of powered versus aero-assisted planetary arrivals are also examined.[61-64] It is assumed that one mission (to Mars and back) occurs once every synodic period. Because Earth-Mars trajectories approximately repeat every seven synodic periods (every 14.95 years), we consider short TOF trajectories over a seven synodic-period cycle (for 2009–2022 Earth departure years).

II. Trajectory Types

A. Direct Transfer (Conjunction Class)

Conjunction class trajectories provide Earth-Mars transfers for three mission scenarios: 1) Direct,[12] 2) Semi-Direct,[13] and 3) Stop-Over.[33] In a Direct mission everything (crew, transfer vehicle, etc.) is launched from Earth's surface directly towards Mars, where the crew and transfer vehicle land via aero-assisted direct entry. After the 500-day Mars stay time everything is launched off of Mars and the crew returns to Earth using direct entry (the transfer vehicle is either landed or expended). The Semi-Direct scenario also begins with all mission components on Earth's surface, but at Mars arrival the transfer vehicle is placed into a parking orbit (either with a powered maneuver or aerocapture) instead of landing on the surface. At Mars departure, the crew rendezvous with the transfer vehicle in orbit then returns to Earth. For Stop-Over missions, the crew begins on Earth, but the transfer vehicle begins in Earth orbit (e.g. from a previous mission). After an in-orbit rendezvous the crew and transfer vehicle leave for Mars, where the crew lands and the transfer vehicle is placed in orbit. Following another in-orbit rendezvous, the crew and transfer vehicle depart for Earth, where the crew lands and the transfer vehicle is placed in Earth orbit for reuse. (A summary of the mission scenarios and trajectories are provided in Table 1.)

A sample mission using direct transfers is illustrated in Fig. 1. This particular scenario begins on September 9, 2022 followed by a 180-day transit to Mars. [All subsequent trajectory plots (Fig. 1–Fig. 5) include an outbound transfer in 2022.] The Mars stay-time is 550 days, and the mission concludes on March 24, 2025 after a 180-day inbound transfer.

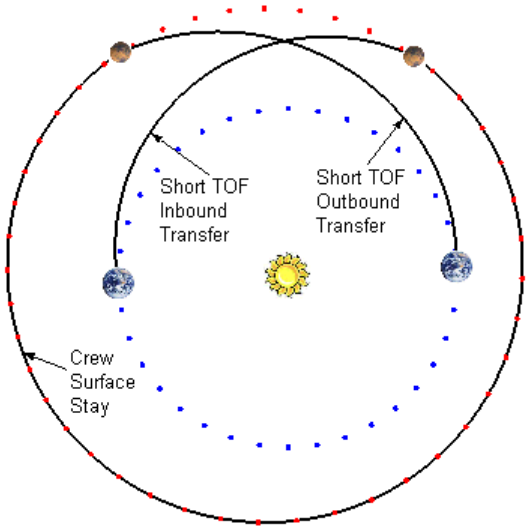

Fig. 1 Outbound and inbound direct transfers.

B. Free-Return

Should an accident on the way to Mars preclude the crew from landing (e.g. a propulsion system failure), a free-return trajectory would allow the crew to return to Earth without any major maneuvering (i.e. zero deterministic ΔV). These trajectories are constructed such that if there is no capture maneuver at arrival, a slight gravity assist

from Mars will send the crew and vehicle back to Earth. We examine free-return trajectories for Direct, Semi-Direct, and Stop-Over mission scenarios, though free-returns may be used (and are often incorporated) in Semi-Cycler and Cycler scenarios. There are three traditional types of Mars free-return trajectories: 1) Opposition/Venus flyby,[41] 2) 1:2 spacecraft:Earth resonance,[39] and 3) 2:3 spacecraft:Earth resonance.[39] For constrained TOF and long duration missions (on the order of three years) the 2:3 resonance free return provides the lowest average ΔV of the three choices, thus we choose to examine this type in more detail. (We note that the Venus flyby free-returns occasionally offer better performance than the 2:3 resonance trajectories, but involve large variations in ΔV over several synodic periods.)

An example 2:3 resonance free-return trajectory is presented in Fig. 2. Because this trajectory was constructed while constraining the Earth-Mars TOF, it no longer adheres to the 2:3 resonance, but still allows a return to Earth with no post-launch ΔV. While the free-return abort is available, the nominal mission only uses the Earth-Mars portion of the trajectory. The crew would stay on Mars for about 550 days then take a short TOF inbound trajectory home (e.g. the Mars-Earth transit in Fig. 1).

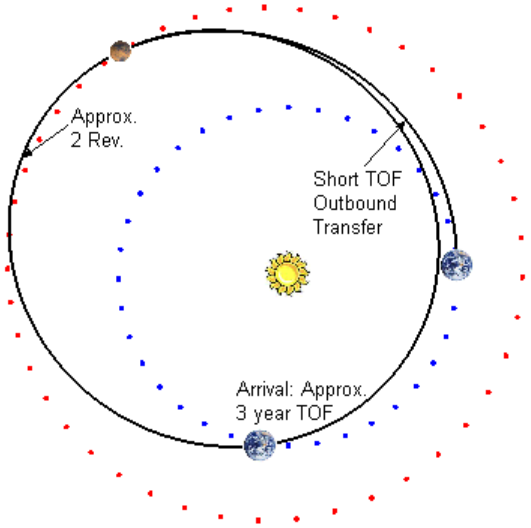

Fig. 2 Mars free-return trajectory.

C. Mars-Earth Semi-Cycler

A transfer vehicle on a Mars-Earth semi-cycler trajectory begins at Mars (ideally in a loose parking orbit), swings by Earth to drop-off the returning crew, reencounters Earth after orbiting the sun (sans crew), then picks up the next Mars-bound crew and stays in orbit about Mars until the next transfer opportunity. Thus the trajectory sequence is Mars-Earth-Earth-Mars. The first trajectory maneuver ejects the transfer vehicle from Mars orbit; no maneuver occurs at Earth arrival (the crew employs aero-entry); a "taxi" vehicle launch transports the crew from Earth to the transfer vehicle (hyperbolic rendezvous); and either a propulsive maneuver or aerocapture achieves Mars orbit insertion. Deep space maneuvers (DSMs) are also often required to maintain the trajectory. We note that one trajectory is used for both the outbound and inbound transfers to reduce the number of required maneuvers (and hence the number of ΔV). For example, only one Mars departure maneuver is necessary when the trajectory incorporates both transfers (i.e. Earth-Mars and Mars-Earth), while two maneuvers are required when the outbound and inbound trajectories are separate.

The total trajectory duration (from Mars launch to Mars arrival) dictates the number of transfer vehicles required to provide one mission per synodic period. For example, if the total interval is between two and three synodic periods then three vehicles would be required to provide short TOF outbound and inbound transfers each synodic period. We examined two-vehicle[42] and three-vehicle[43] trajectories and found the average ΔV to be comparable, so we choose the two-vehicle option to reduce cost. There are three types of two-vehicle trajectories that can be distinguished by the Earth-Earth transfer: 1) near 1:2 resonance, 2) near 3:2 resonance, and 3) 1.5-year inclined transfer (with an extra Earth flyby). These three trajectory types are depicted in Fig. 3. The first leg (Mars-Earth) of the trajectory provides the return trip for a mission launched in the previous synodic period. (In the case of Fig. 3 the trajectories begin in 2020, supplying the return for a mission launched from Earth in 2018.) After the Earth-

Earth transfer, a new mission begins with a crew transfer to Mars on the final leg of the trajectory (for the 2022 outbound opportunity). We find that the near 1:2 resonance type provides the lowest ΔV Mars-Earth semi-cycler when Mars is near perihelion (during the 2018–2022 Earth-Mars opportunities); the near 3:2 resonance type is most effective when Mars is near aphelion; and the 1.5 year type is best for the longer TOF transfers (when TOF > 230 days). Though the 3:2 resonance type has a perihelion well within Venus's orbit (see Fig. 3b), the crew will not be on the transfer vehicle at this point, so they would avoid extra radiation exposure.

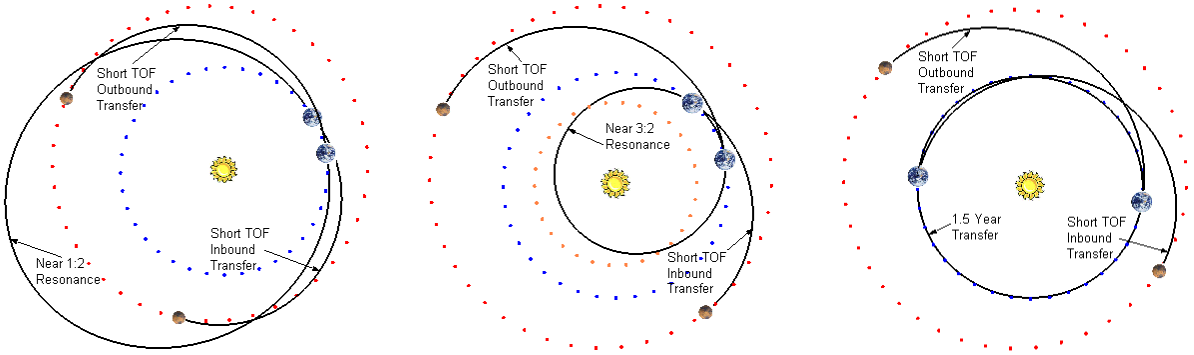

a) near 1:2 resonance version **b) near 3:2 resonance version** **c) 1.5 year transfer version**

Fig. 3 Mars-Earth semi-cyclers.

D. Earth-Mars Semi-Cycler

This trajectory is the opposite of the Mars-Earth semi-cycler; instead of Mars-Earth-Earth-Mars, the sequence is Earth-Mars-Mars-Earth. The maneuver sequence is thus: transfer vehicle Earth-orbit departure, crew aero-entry at Mars, crew taxi launch and hyperbolic rendezvous with the transfer vehicle at Mars, then propulsive or aerocapture Earth arrival. Additional transfer vehicle DSMs are usually necessary. We identified two classes of Earth-Mars semi-cyclers: 1) three-vehicle (the trajectory duration is between two and three synodic periods) and 2) four-vehicle (the total duration is between three and four synodic periods). One version of three-vehicle trajectory is based on the trajectory discussed in Ref. 48, which has a short TOF Earth-Mars transfer followed by a 3:2 resonance orbit with Mars then another short TOF transfer back to Earth. The other three-vehicle trajectory begins with a 1:2 resonance free-return trajectory (with short Earth-Mars TOF), then an Earth gravity assist places the spacecraft into a 1:1 resonance orbit and another 1:2 resonance free-return (with short Mars-Earth TOF) completes the trajectory. (This flyby sequence is Earth-Mars-Earth-Earth-Mars-Earth.) We also examined two versions of four-vehicle Earth-Mars semi-cyclers. The first version employs a short Earth-Mars leg, then a near 4:3 Mars resonance orbit, followed by a short Mars-Earth transfer (as in Fig. 4a). The second version begins with a 2:3 resonance free-return trajectory (with short Earth-Mars TOF), followed by a 1:1 resonance with Earth and another 2:3 resonance free-return provides a short TOF transfer from Mars to Earth (as in Fig. 4b). So, these semi-cyclers are either constructed from a resonant Mars orbit bounded by short TOF legs, or from two free-returns (one outbound, one inbound) connected by a one-year Earth-Earth transfer.

We propose these four-vehicle trajectories for Earth-Mars semi-cycler missions because the ΔV requirements (which correlate to mass and cost) are significantly lower than the three-vehicle ΔV. (Thus four relatively small transfer vehicles are chosen over three large ones.) The free-return semi-cycler is most effective for short transfers (when TOF < 150 days) and when Mars is near aphelion (during the 2009 and 2022 outbound opportunities), while the near 4:3 resonance semi-cycler is best for longer TOF transfers. Fig. 4 presents an example of both four-vehicle trajectory versions.

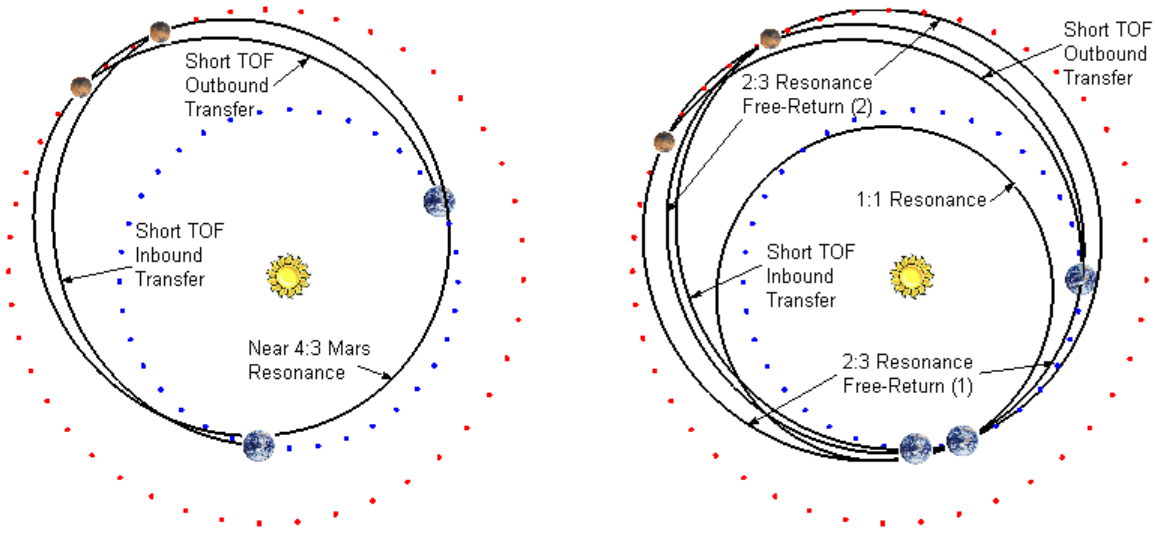

a) near 4:3 resonance version **b) free-return version**

Fig. 4 Earth-Mars semi-cyclers.

E. Cycler

Cycler trajectories encounter Earth and Mars on a (nearly) regular basis, but do not stop at either planet (i.e. they continue in orbit about the sun indefinitely). The main maneuvers in a cycler mission are crew taxi launches at Mars and Earth to rendezvous with the transfer vehicle plus any DSMs required to maintain the cycler orbit. Because the crew lands via direct entry and the transfer vehicle never enters a parking orbit, there is no ΔV cost for planetary arrivals. We examined two-vehicle,[46] three-vehicle,[48] and four-vehicle cyclers[47,49] and we found the latter variety to require the least ΔV, which makes them attractive for use in Mars missions. (Again, the initial investment of launching extra vehicles results in lower mass missions.) An example outbound cycler trajectory is given in Fig. 5, where we note that the cycle is a repitition of the sequence Earth-Mars-Earth (so we have EME EME…). There is also a corresponding inbound cycler, which provides short TOF Mars-Earth transfers.

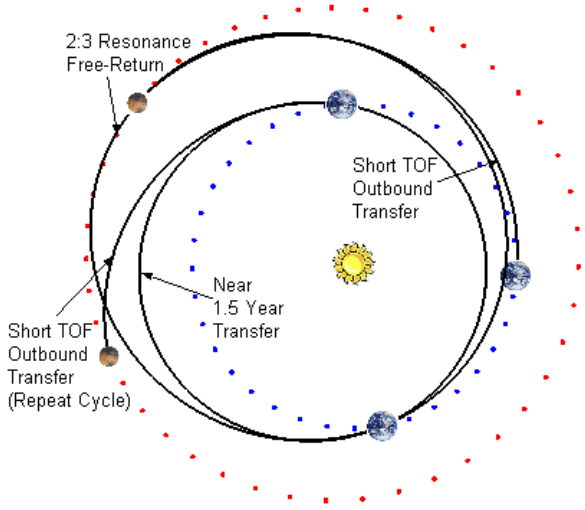

Fig. 5 Outbound cycler trajectory.

Table 1 Summary of Earth-Mars mission scenarios

	Earth Encounter	Mars Encounter	Schemata
Direct	Surface	Surface	
Semi-Direct	Surface	Parking Orbit	
Stop-Over	Parking Orbit	Parking Orbit	
M-E Semi-Cycler	Flyby	Parking Orbit	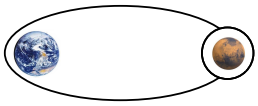
E-M Semi-Cycler	Parking Orbit	Flyby	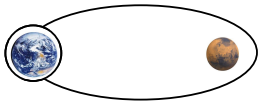
Cycler	Flyby	Flyby	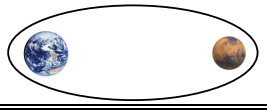

III. Trajectory Models

We model the heliocentric trajectories as point-to-point conics with instantaneous $\mathbf{V}_\infty$ rotations at planetary encounters. The minimum allowable flyby altitude at Earth and Mars is 300 km. Deep space maneuvers are also modeled as instantaneous changes in the heliocentric velocity. We do not allow maneuvers within the sphere of influence of a flyby planet because of the operational difficulty in achieving an accurate $\mathbf{\Delta V}$ during a gravity assist. We assume that planetary departure and arrival maneuvers occur at 300 km above the planet's surface, thus the ΔV for escape or capture is

$$\Delta V = \sqrt{V_\infty^2 + 2\mu / r_p} - \sqrt{2\mu / r_p} \tag{1}$$

where μ is the gravitational parameter of the planet and r_p is the periapsis radius of the escape or capture hyperbola (in this case 300 km above the surface radius). While Eq. (1) is explicitly the ΔV to achieve a $\mathbf{V}_\infty$ magnitude from a parabola, it is sufficient to optimize interplanetary transfers that begin on the surface or in a parking orbit. The difference between the true ΔV and Eq. (1) is found by subtracting the launch trajectory or parking orbit velocity at r_p from the periapsis velocity of the parabola. Because this difference is independent of the interplanetary transfer (both the parking orbit and the parabola are planetocentric trajectories), it does not affect the outcome of the optimal trajectory.

The sequence of maneuvers included in the optimal ΔV calculation is summarized in Table 2 for each trajectory type. If the crew taxi, transfer vehicle (TV), or both vehicles performs a maneuver (when the maneuvers are required is provided in Table 2), the weighting on the corresponding ΔV is unity, and if no maneuver is performed then the weighting is zero. Throughout this paper we assume the semi-cycler or cycler transfer vehicle is already in a parking orbit or on an interplanetary trajectory; thus, we ignore the initial transfer vehicle launch cost for these trajectories. While these relative weightings (one or zero) do not explicitly minimize mission mass or cost, the resulting trajectories are representative of those that result from more detailed analyses (e.g. one that includes the vehicle masses). A key benefit of our weighting system is that we only rely on natural parameters (planetary orbits and masses) for computations, yet we retain trajectory features (i.e. low V_∞ and low ΔV) that are essential for effective integrated mission design.

Table 2 Required maneuvers for each trajectory type

	Earth departure ΔV	Mars arrival ΔV	Mars departure ΔV	Earth arrival ΔV	DSM
Direct	taxi & TV	TV[a] neither[b]	taxi & TV	TV[a] neither[b]	neither
Free-return	taxi & TV	TV[a] neither[b]	N/A	N/A	neither
Mars-Earth semi-cycler[c]	taxi	TV[a] neither[b]	taxi & TV	neither	TV
Earth-Mars semi-cycler[c]	taxi & TV	neither	taxi	TV[a] neither[b]	TV
Cycler[c]	taxi	neither	taxi	neither	TV

[a]Powered capture.
[b]Aero-assisted capture.
[c]The one-time transfer vehicle launch ΔV is ignored.

Low-thrust trajectory legs are modeled as a series of constrained ΔVs, which mimics the effect of continuous low-magnitude acceleration.[59] We compute direct (Earth-Mars and Mars-Earth) low-thrust trajectories for both powered and aero-assisted arrivals with the objective of maximizing the final mass of the spacecraft. The initial spacecraft state is the position and velocity of the departure planet. The target planet's position and velocity are matched for powered arrivals (thus $V_\infty = 0$), but only the position is matched for aero-arrivals (where $V_\infty \neq 0$). The planetocentric portion of the trajectory is assumed to be fixed (i.e. we assume the spacecraft is launched optimally off the surface to reach $V_\infty = 0$), though better performance is possible when both the planetocentric and heliocentric portions are optimized as a whole trajectory.[60] Again, these low-thrust trajectories do not necessarily minimize mission cost, but are indicative of the type of trajectory that would optimize a human mission to Mars.

We use a sequential quadratic programming algorithm[65,66] to compute minimum-ΔV (or maximum final mass for low-thrust) trajectories with bounded TOF. (By bounded we mean the TOF may be less than or equal to the constrained value.) Similar methods have been used in the optimization of the Galileo trajectory to and at Jupiter and the Cassini trajectory to Saturn.[67, 68] We optimize Earth-Mars trajectories so that the total ΔV over the entire 15-year cycle is minimized (as opposed to, say, minimizing the maximum ΔV during the cycle). Though the arrival V_∞ for aerocapture is often limited (e.g. below 9 km/s at Earth[62] and below 7 km/s at Mars[63]), we did not constrain the V_∞; in this way we analyze the lowest possible ΔV trajectories. An initial guess for the timing and placement of DSMs is obtained via Lawden's primer vector analysis.[69, 70] For each trajectory type, we initially optimized the long TOF (270-day) trajectory for the 2009 outbound opportunity. The 270-day TOF trajectory served as the initial guess for the 260-day TOF trajectory, and so on (by 10-day intervals) until the 120-day TOF transfer was optimized. The whole process was then repeated for the subsequent synodic periods up to the 2022 outbound opportunity. In the case of cyclers, multiple synodic periods were optimized together because the trajectory is continuous. We employed a similar process from 120-day to 270-day TOF (and vice-versa) to optimize the semi-cycler and cycler trajectories.

IV. Results

A. Impulsive ΔV transfers

The optimal ΔV for a given TOF fluctuates significantly over the seven synodic-period cycle (about 15 years) due to the eccentricity and inclination of Mars' orbit. Usually, the largest-ΔV missions occur when Mars is near aphelion (during the 2009 opportunity), and the smallest-ΔV missions occur when Mars is near perihelion (during the 2016 opportunity). For a given TOF, the maximum-ΔV mission corresponds to the smallest Mars payload mass, while the minimum-ΔV mission provides an opportunity to send the most payload to Mars. Alternatively, the maximum-ΔV mission indicates the longest TOF necessary to land a given payload at Mars, while the minimum-ΔV opportunity sets the lower bound on TOF over the synodic-cycle. Because the mission requirements fluctuate significantly over the 15-year cycle, we provide trajectory data for each of the seven launch opportunities (2009–2022) as well as the average and maximum values. The average values provide an estimate of the mission cost over several synodic periods, while the maximum trajectory values set an upper-bound for the design of mission components. For example, the maximum Earth-departure V_∞ would size the launch vehicle upper-stage, and the

maximum Mars arrival V_∞ would size the heat shield or propulsive-capture system at Mars. We note that the maximum trajectory requirements do not generally occur during the same launch opportunity; thus they are better suited to the design of mission components rather than an analysis of comprehensive mission scenarios.

The key mission parameters include: the optimal total ΔV, the arrival and departure V_∞ at Earth and Mars, the DSM ΔV, the Mars stay time, and the total mission duration. These eight parameters are plotted as functions of the maximum allowable TOF in Fig. 6–Fig. 8 (which provide average performance) and in Fig. 9–Fig. 11 (which provide maximum values). These average and maximum values are derived from the Earth-Mars trajectories that span the seven launch opportunities between 2009 and 2022 (given in the appendix, where we provide Fig. 15–Fig. 35). We compute the root-mean-square of the V_∞ in Fig. 8 because it leads to a better estimate of the average mission ΔV than the V_∞ mean. There is an ambiguity in how to charge the DSM ΔV in semi-cycler and cycler trajectories because these trajectories span multiple synodic periods (e.g. an Earth-Mars semi-cycler starting in 2009 flys by Mars twice and returns to Earth in 2016, spanning three synodic periods). To resolve this ambiguity, we allocate the Earth-Mars semi-cycler DSM ΔV to the mission that the Earth-Mars leg initiates, and the Mars-Earth semi-cycler DSM ΔV is charged to the mission that the Mars-Earth leg concludes. (Thus any DSMs that occur between 2009 and 2016 for an Earth-Mars semi-cycler are charged to the 2009 mission.) In the case of cyclers, we resolve the ambiguity as follows: any cycler DSMs that occur between the Earth encounters that precede or follow a crew transfer leg (Earth-Mars or Mars-Earth) are allocated to that mission.

The thin black lines and the thick gray lines in Fig. 6–Fig. 11 and in the appendix (i.e. Fig. 15–Fig. 35) denote the powered or aero-assisted capture option in Table 2, respectively. A sharp jump (a vertical line) in the data indicates a shift in trajectory type. For example, the change in ΔV from 3 km/s to 4 km/s at 190 days TOF for the aero-assisted Earth-Mars semi-cyclers in Fig. 9a is a result of the optimal outbound trajectory switching from the near 4:3 resonance version (Fig. 4a) to the free-return version (Fig. 4b) in 2009 (as also shown in Fig. 15a). A horizontal line indicates that the optimal trajectory is no longer constrained by the TOF bound (e.g. TOF = 220 through 270 days for powered free returns in Fig. 9a) and the optimal TOF is below the allowable limit.

While the total ΔV is the key factor for optimization, the other trajectory parameters provide additional insight for analyzing Mars mission scenarios.

As an example, we examine the average cycler mission with the TOF constrained below 210 days. For cycler missions the escape energy required by the crew taxi to rendezvous with the cycling transfer vehicle depends on the departure V_∞ [5.0 km/s at Earth (Fig. 8a) and 3.3 km/s at Mars (Fig. 8c)]. The arrival V_∞ [5.8 km/s at Mars (Fig. 8b) and 5.8 km/s at Mars (Fig. 8d)] size the heat shield that decelerates the taxi to a safe surface landing. The DSM ΔV [0.78 km/s (Fig. 6b)] indicates the propulsion system requirements of the transfer vehicle. Finally, the Mars stay time [560 days (Fig. 7a)] provides a time allotment for surface exploration, and the mission duration [915 days (Fig. 7b)] determines the time that the crew spends away from Earth and the amount of consumables needed to sustain them. Similarly, other mission scenarios may be examined by applying the corresponding trajectory data in Fig. 6–Fig. 11 and in the appendix.

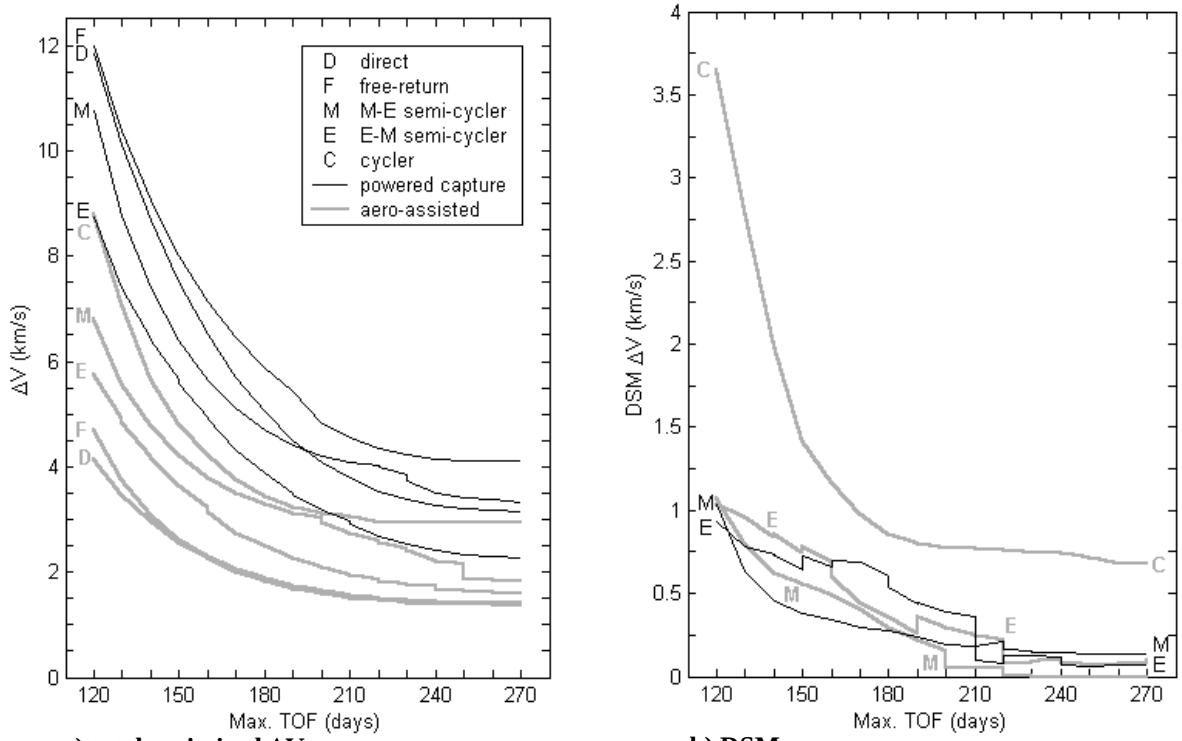

a) total optimized ΔV **b) DSM**

Fig. 6 Average Δ*V* over 15-year cycle.

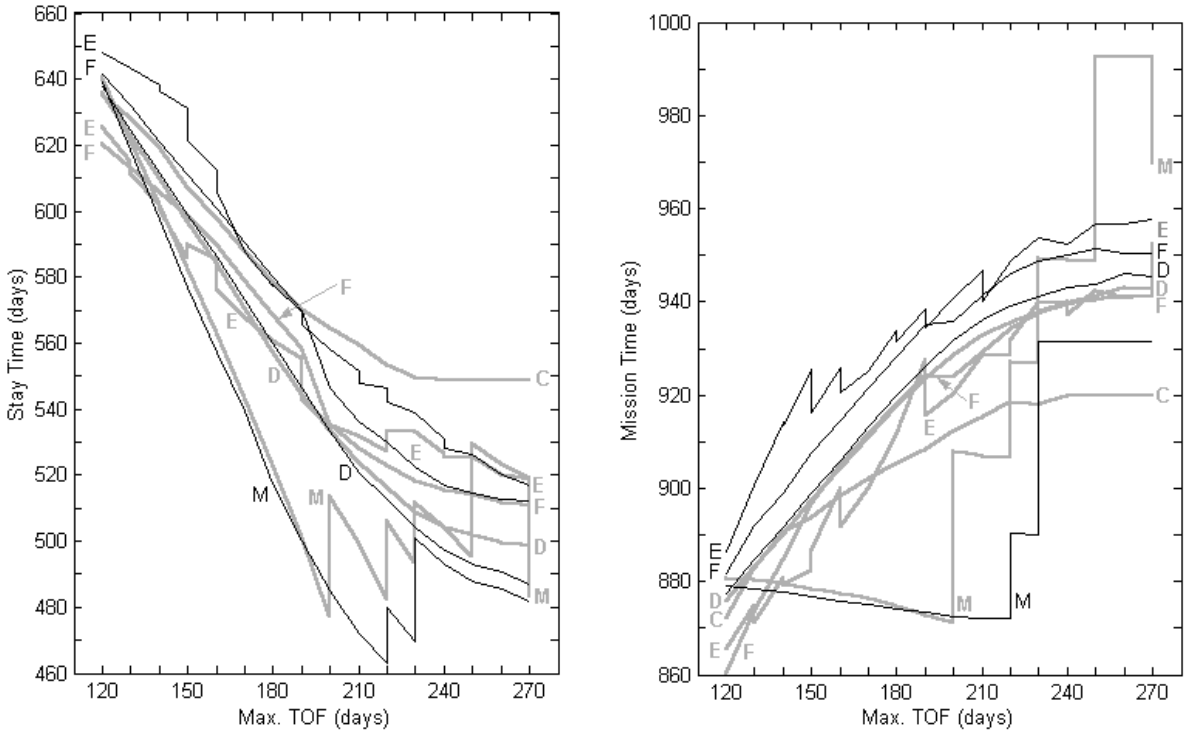

a) Mars stay time **b) total mission duration**

Fig. 7 Average stay time and mission time over 15-year cycle.

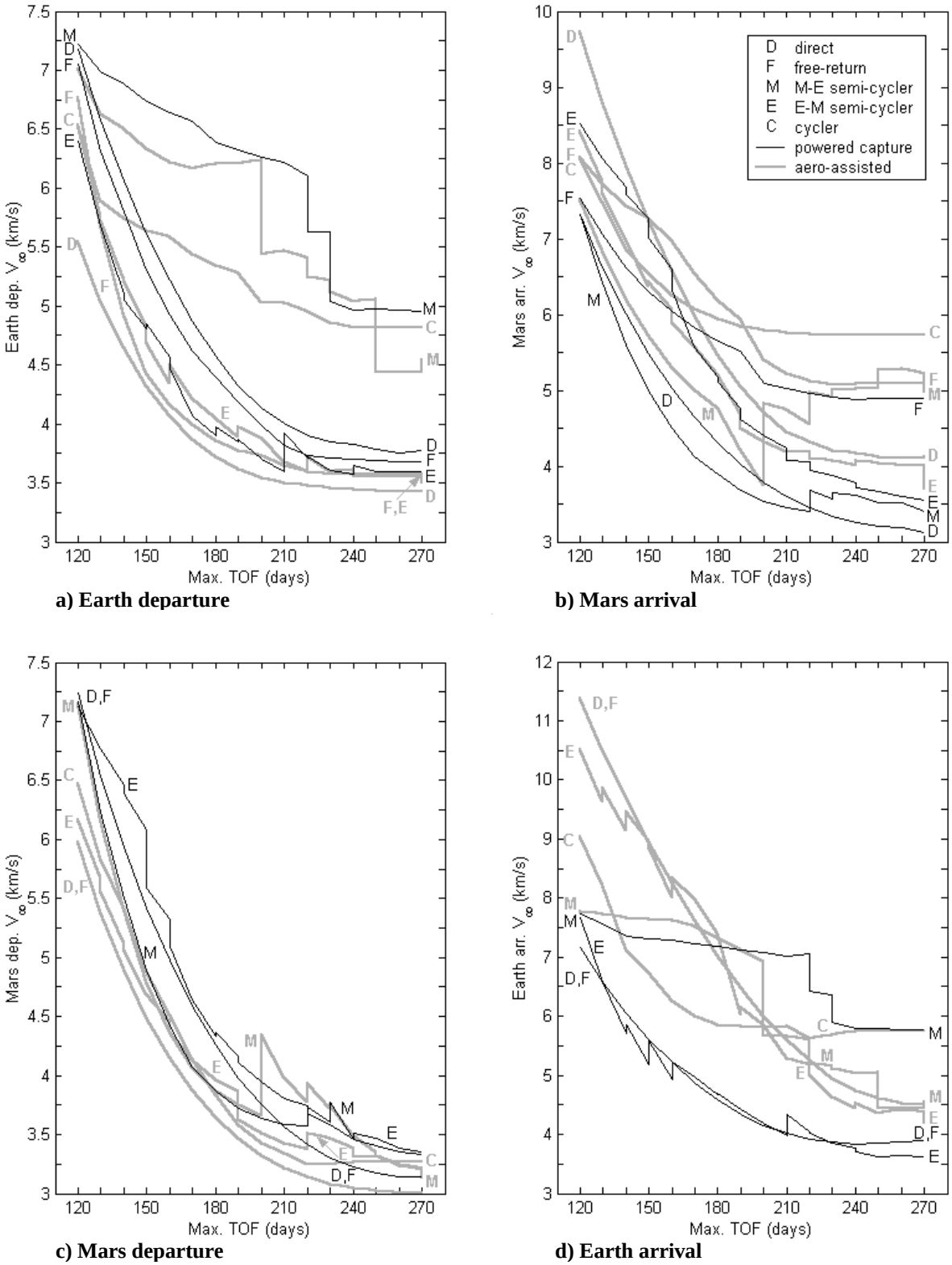

a) Earth departure **b) Mars arrival**

c) Mars departure **d) Earth arrival**

Fig. 8 Root-mean-square V_∞ over 15-year cycle.

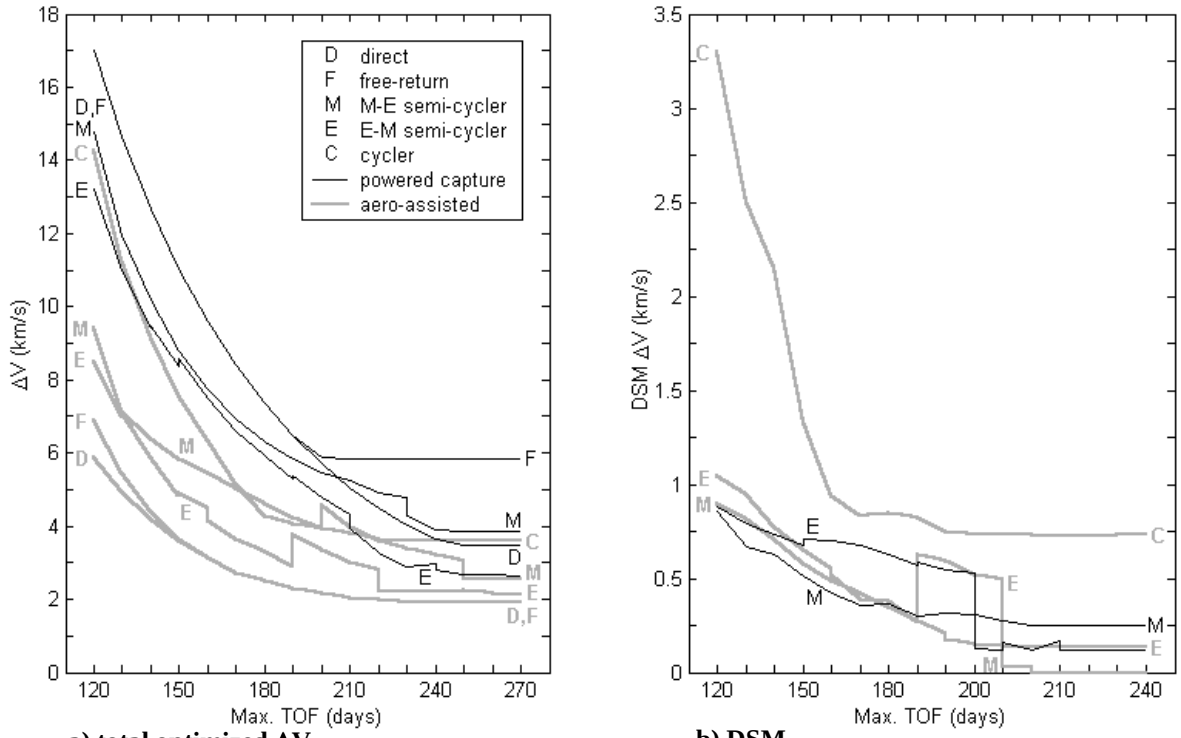

a) total optimized ΔV **b) DSM**

Fig. 9 Maximum Δ*V* over 15-year cycle.

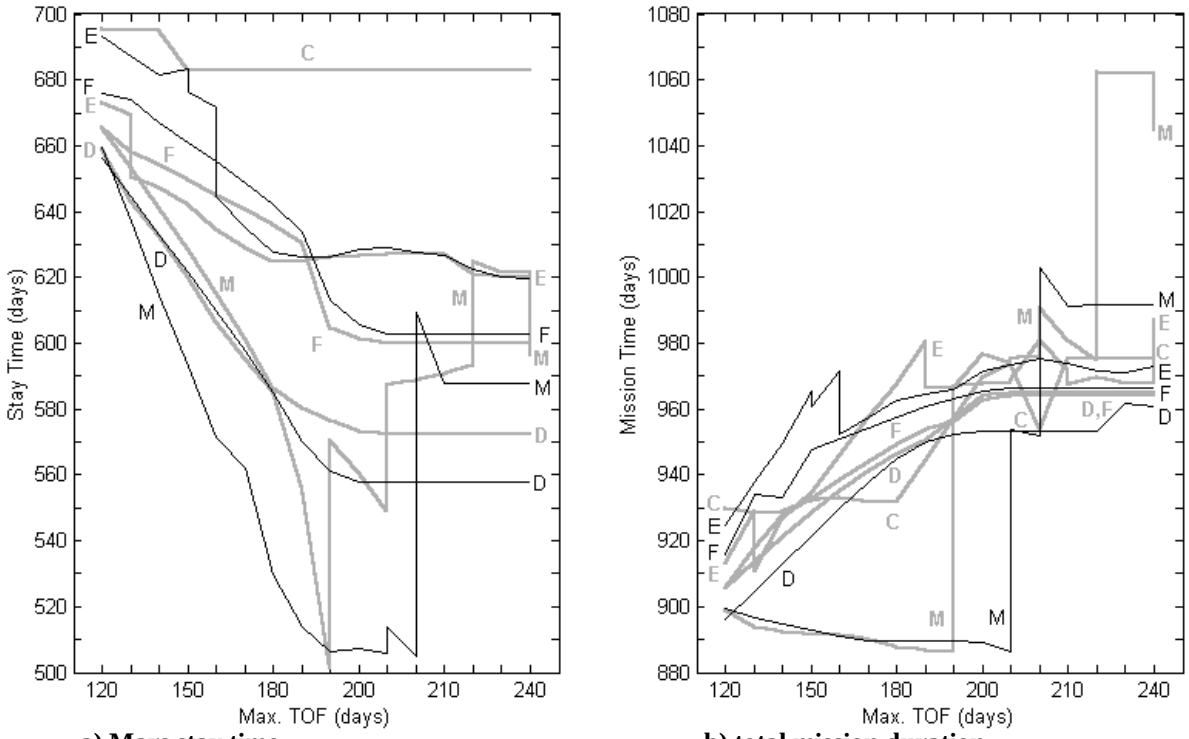

a) Mars stay time **b) total mission duration**

Fig. 10 Maximum stay time and mission time over 15-year cycle.

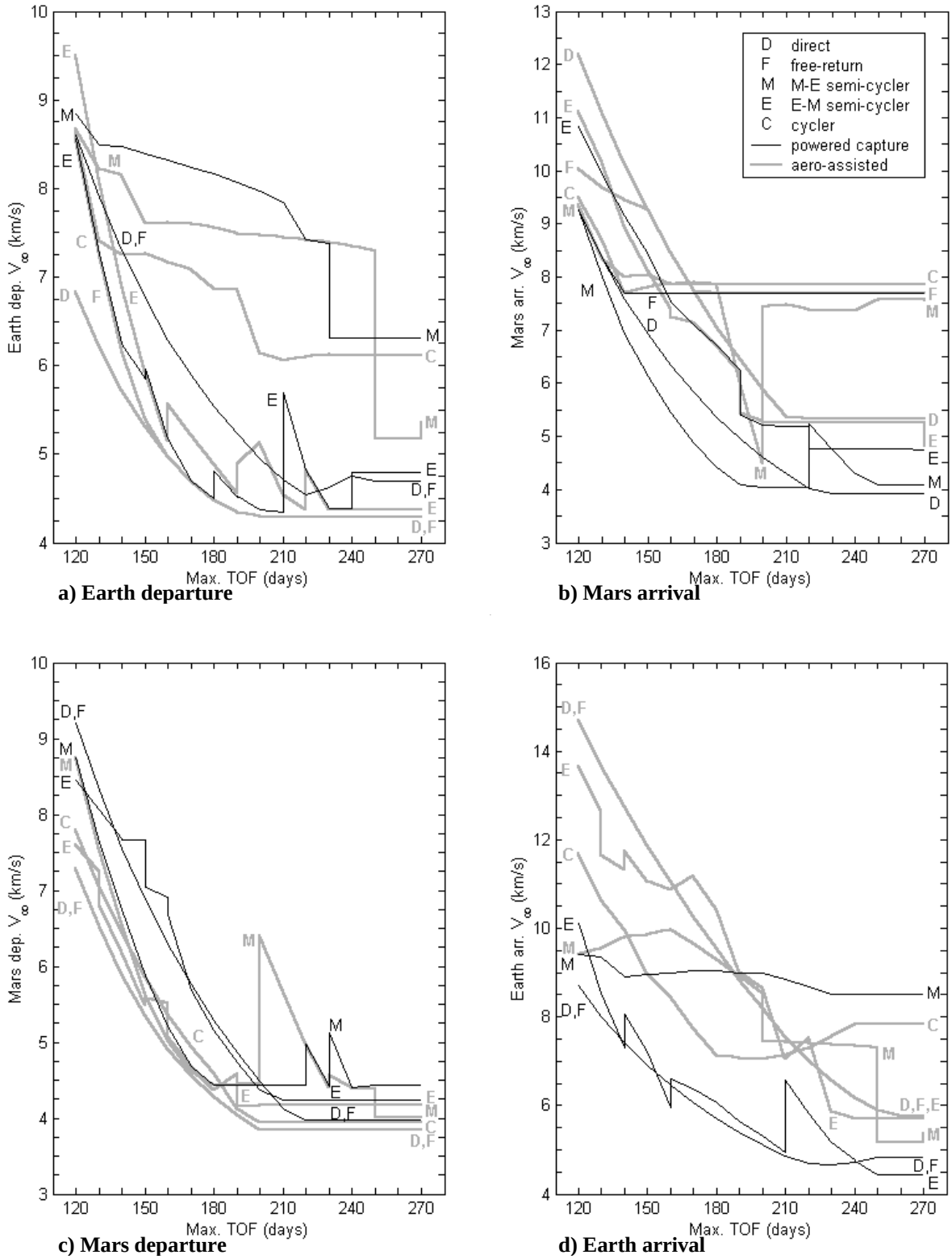

a) Earth departure **b) Mars arrival**

c) Mars departure **d) Earth arrival**

Fig. 11 Maximum V_∞ over 15-year cycle.

The variation in total ΔV (e.g. Fig. 6a) among the trajectory types is mainly attributed to the different number of maneuvers in the cost function (summarized in Table 2). For example, powered-capture direct trajectories have four maneuvers in the ΔV calculation (Earth departure, Mars arrival, Mars departure, and Earth arrival), while aero-assisted capture direct trajectories include only two maneuvers (Earth departure and Mars departure). In fact, all of the aero-assisted capture trajectories share the same cost function (Earth and Mars departure plus DSM ΔV). Usually, the ΔV-rank order (from lowest to highest) is direct, free-return, Earth-Mars semi-cycler, Mars-Earth semi-cycler, then cycler.

The powered-capture direct and free-return trajectories also share identical cost functions and their ΔV are nearly identical except during the 2014 (for TOF above 180 days), 2016, and 2018 (for TOF below 200 days) launch opportunities. The key reason for the difference in ΔV (between direct and free-return trajectories) is that the Mars-flyby V_∞ must be relatively high to complete the free return to Earth (with no DSMs). In fact, during the 2016 launch opportunity the V_∞ is never below 7.5 km/s. To account for the higher Mars V_∞, the Earth-departure V_∞ are usually lower for free returns than for direct trajectories. On the other hand, aero-assisted trajectories do not include the arrival V_∞ in the ΔV-cost function, and the direct and free-return average ΔV is within a few percent, especially when the TOF is greater than 150 days. As a result, incorporating the free-return abort option in a human mission to Mars with direct aero-entry does not change the ΔV requirements significantly, yet reduces the risk to the crew. The main disadvantage of these free-return trajectories is that, in the event of abort, the crew does not return to Earth until after 1,080 days i.e. three years (on average) instead of the 930-day nominal mission duration.

In comparison to the other trajectory types, optimal Mars-Earth semi-cyclers tend to have higher Earth V_∞ and lower Mars V_∞, while the V_∞ of Earth-Mars semi-cyclers are closer to the direct counterparts (within 10% on average). The cycler Earth-departure V_∞ are usually much larger (around 40% greater) than the direct case, but the Mars-departure V_∞ are often much lower (only 5% above the direct V_∞)—primarily because of DSMs that precede the Mars flyby. Because the cycler-arrival V_∞ do not vary as a function of TOF as much as the direct trajectories do, the arrival V_∞ for cyclers are significantly lower (by about 20%) for short TOF and are much higher (by about 30%) for long TOF when compared to the direct V_∞. Often, the Earth-Mars semi-cycler DSM ΔV are larger than the Mars-Earth semi-cycler DSM ΔV for short TOF, and are slightly lower for long-TOF trajectories. The cycler DSM ΔV are significantly larger than (i.e. at least double) the DSM ΔV of semi-cyclers. The Mars stay time and total mission duration do not vary significantly among the trajectory types (for a given transfer TOF) with the exception of Mars-Earth semi-cyclers, which have notably lower stay times and mission durations for low to moderate TOF and have mission durations in excess of 1,000 days for TOF above 240 days during the 2016 and 2020 launch opportunities. Also, cyclers tend to have slightly longer stay times (an average of 50 days longer) than the other optimized trajectories.

The fundamental advantage of aero-assisted capture is that a heat-shield is often considerably less massive than the propellant required to decelerate a vehicle at planetary arrival. As a result, less mass must be launched from Earth, which ultimately reduces mission cost. A secondary benefit of direct entry or aerocapture is that the departure V_∞ is reduced significantly below the powered capture case (at the expense of higher arrival V_∞). For example, direct and free-return departure V_∞ for aero-assisted trajectories range from about 20% (for short TOF) to 10% (for long TOF) below the powered capture V_∞ at either Earth or Mars. However, this benefit becomes less pronounced for short TOF trajectories if arrival-V_∞ limits are required (to satisfy entry guidance and heating constraints), but the combination of negligible propellant cost at arrival and reduced departure energy still provides a distinct advantage over powered capture missions. The V_∞ reduction is not as prominent for semi-cycler trajectories, which always have at least one aero-arrival. (Mars-Earth semi-cyclers employ direct entry at Earth and Earth-Mars semi-cyclers employ direct entry at Mars.) As a result, the Mars-departure V_∞ for Mars-Earth semi-cyclers and the Earth-departure V_∞ for Earth-Mars semi-cyclers do not change significantly between aero-assisted and powered-capture trajectories. There is a notable difference on the other short TOF transfer, where the Earth-departure V_∞ for Mars-Earth semi-cyclers is reduced by 10% (on average) and the Mars-departure V_∞ for Earth-Mars semi-cyclers decreases by 10%–20% when comparing the aero-assisted to the powered-capture trajectories. In our formulation, powered arrivals are not necessary for cycler missions; thus, there is no distinction between aero-assisted and powered cycler trajectories.

As expected, the optimal ΔV and V_∞ decrease as the TOF upper limit is increased, and the stay time decreases and the mission duration increases as the TOF becomes larger. We note that the ΔV increases dramatically for short TOF trajectories. For example, the ΔV for most trajectories doubles from 270-day TOF to 150-day TOF, then triples (with respect to 270-day TOF) at TOF of only 130 days. Notable exceptions include direct and Earth-Mars semi-cycler powered-capture trajectories, which double around 180-day TOF and triple at 150-day TOF for the

maximum-ΔV transfers. Consequently, the same amount of ΔV is saved by extending the TOF by 20 days from 130- to 150-day TOF as is saved by allowing the TOF to increase by 120 days from 150- to 270-day TOF, on average.

Further, when the maximum TOF is extended from 180 days up to 270 days, the relative ΔV savings range from 15%–45% for average missions, and up to 65% of the ΔV is eliminated for the maximum-ΔV missions (which are usually during the 2009 or 2022 launch opportunities). Alternatively, the absolute reduction in ΔV (from 180- to 270-day TOF) is around 1.5 km/s for powered capture and 0.75 km/s for aero-assisted capture, with up to 4 km/s reduction in the maximum ΔV. Also, the average ΔV reduction is 10%–20% when the TOF is extended by only 30 days from 180 days to 210 days, which translates to an absolute ΔV savings of around 1 km/s for powered capture and 0.4 km/s for aero-assisted trajectories with up to a 2 km/s reduction in the maximum ΔV. We note that the ΔV savings is usually much less during opportunities when Mars is near perihelion (namely 2016–2018).

The maximum-departure V_∞ for aero-assisted direct trajectories (Fig. 11a for Earth and Fig. 11c for Mars) establish a lower bound on the V_∞ required to reach Mars from Earth (or vice-versa) for every launch opportunity. For example, the maximum Earth-departure V_∞ for 180-day TOF is 4.5 km/s. If an upper-stage for Mars missions only provides an excess velocity of 4.3 km/s for a given payload, then the nominal mission is not always available; either the payload must be reduced or the TOF must be extended (at the expense of some additional shielding or artificial gravity) during the more demanding launch years (in this case 2009 and 2022). Similar lower bounds may be determined for any desired TOF between 120 and 270 days using the aero-assisted direct-trajectory curves in Fig. 11.

Though semi-cycler and cycler trajectories typically require higher V_∞ and higher ΔV than direct trajectories, the mass requirements (e.g. initial mass in low-Earth orbit or total propellant mass) for semi-cycler and cycler missions are generally lower because the relatively massive transfer vehicle (which contains radiation shielding, interplanetary life-support systems, crew accommodations, etc.) performs fewer maneuvers.[16] (Again, we ignore the one-time cost of launching a semi-cycler or cycler transfer vehicle. For example direct, semi-direct, and stop-over missions (which are summarized in Table 1) are constructed so that the transfer vehicle performs between two to four maneuvers (as given in Table 2), while semi-cycling transfer vehicles perform two to three maneuvers and cycler vehicles perform only one. [The transfer vehicle requirements are even less for ballistic (DSM $\Delta V = 0$) trajectories.] In essence, more of the mission ΔV is executed by the crew taxis in semi-cycler and cycler missions than with missions that incorporate direct trajectories. As a result, less dry mass (from the transfer vehicle) and less propellant mass (from the elimination of maneuvers) is launched from Earth or Mars, and smaller (or fewer) launch vehicles and upper stages are required to complete the mission. The net mass savings depends on several design factors, but the data compiled in Fig. 6–Fig. 11 and in the appendix provide the basic trajectory characteristics necessary for mission analyses and trade studies.

B. Low-Thrust Transfers

The ΔV required to match the heliocentric orbit of Mars from the orbit of Earth (and vice-versa) using the minimum possible thrust is presented in Fig. 12 for launch years 2009–2022. Because the thrust is minimized, the burn time for these trajectories is equal to the TOF (i.e. the thruster is always on). We found that the ΔV is nearly constant (within 3% of the values in Fig. 12) over a wide range of I_{sp} when the TOF and burn time are fixed. (In the specific case of Fig. 12 we set the mass flow rate to zero or, equivalently, used an infinite I_{sp}.) The final-to-initial mass fraction may be computed for low-thrust missions via the rocket equation[71]

$$\Delta V = \int_0^{t_b} a\,dt = \int_0^{t_b} \frac{T}{m_0 - \dot{m}t}\,dt = \int_0^{t_b} \frac{\dot{m} g I_{sp}}{m}\,dt = -g I_{sp} \ln\left(\frac{m_0 - \dot{m}t_b}{m_0}\right) \tag{2}$$

The mass ratio may be written explicitly as:

$$\frac{m_f}{m_0} = e^{-\Delta V / g I_{sp}} \tag{3}$$

where we assume that the thrust and specific impulse are constant and that the thrust may be computed by

$$T = \dot{m} g I_{sp} \tag{4}$$

Equation (3) may be rearranged to yield an expression for the required thrust for a given I_{sp} and optimal ΔV (for a given TOF and burn-time)

$$\frac{m_f}{m_0} = \frac{m_0 - \dot{m}t_b}{m_0} = 1 - \frac{T t_b}{m_0 g I_{sp}} = e^{-\Delta V / g I_{sp}} \tag{5}$$

so that

$$T = \frac{m_o g I_{sp}}{t_b}\left(1 - e^{-\Delta V / g I_{sp}}\right) \tag{6}$$

In the minimum-thrust case $t_b = \mathrm{TOF}$, thus

$$T = \frac{m_o g I_{sp}}{\mathrm{TOF}}\left(1 - e^{-\Delta V / g I_{sp}}\right) \tag{7}$$

where ΔV as a function of TOF is provided in Fig. 12 and the initial mass and I_{sp} are mission design variables. As an example, we consider a 210-day Earth-to-Mars transfer in 2014 with a transfer vehicle mass at Earth escape (m_0) of 60 mt and an electric propulsion system with an I_{sp} of 3,000 s. From Fig. 12 the required ΔV is 17.0 km/s and the minimum possible thrust to complete the transfer is 42.7 N [from Eq. (7)]. If a state-of-the-art propulsion system only produces 30 N of thrust (at 3,000-s I_{sp}) then a longer flight time (260 days) or a reduction in payload would be necessary to complete a Mars mission that year. On the other hand, a higher thrust level would allow a reduction in TOF or an increase in the delivered payload.

We also examined minimum-thrust transfers for aerocapture missions (for arrival $V_\infty \neq 0$) but found that the V_∞ at arrival was impractical (i.e. it is often at least double the impulsive transfer V_∞). Instead, we optimized low-thrust trajectories with infinite I_{sp} and set the thrust to the levels found in Fig. 12 for a given launch year and TOF combination. The resulting ΔV and arrival V_∞ (where the launch V_∞ is zero) are found in Fig. 13 and Fig. 14, respectively. Equation (5) is still applicable in this situation, and because the same thrust level was used to calculate the powered and aero-assisted capture trajectories, $t_b = \left(\Delta V_A / \Delta V_P\right)\mathrm{TOF}$, thus

$$T = \frac{\Delta V_P}{\Delta V_A}\frac{m_o g I_{sp}}{\mathrm{TOF}}\left(1 - e^{-\Delta V_A / g I_{sp}}\right) \tag{8}$$

where ΔV_P is the powered arrival ΔV (from Fig. 12) and ΔV_A is the aero-arrival ΔV (from Fig. 13). If we again consider a 210-day transit in 2014 with a 60 mt vehicle and an I_{sp} of 3,000 s, then a thrust level of 53.3 N provides a transfer with a ΔV of 3.17 km/s and 6.16 km/s arrival V_∞ (from Fig. 13 and Fig. 14). The arrival V_∞ are also nearly constant over a range of I_{sp} (and constant burn time) with a variation within approximately 5% of the values found in Fig. 14. We note that increasing the thrust magnitude will decrease the ΔV and burn time, and in the limit of infinite thrust and zero burn time, the ΔV approaches the sum of the departure and arrival V_∞ for powered capture missions and becomes the departure V_∞ for aero-assisted capture.

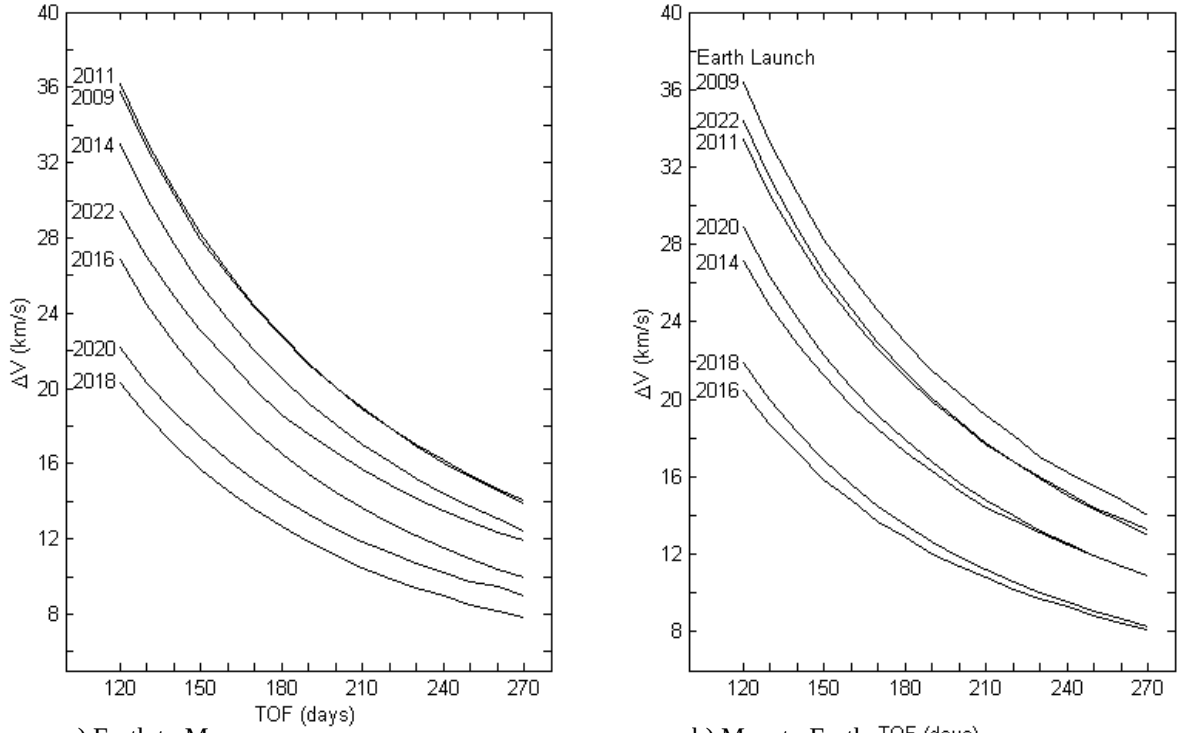

a) Earth to Mars b) Mars to Earth

Fig. 12 ΔV for minimum-thrust transfers with powered capture.

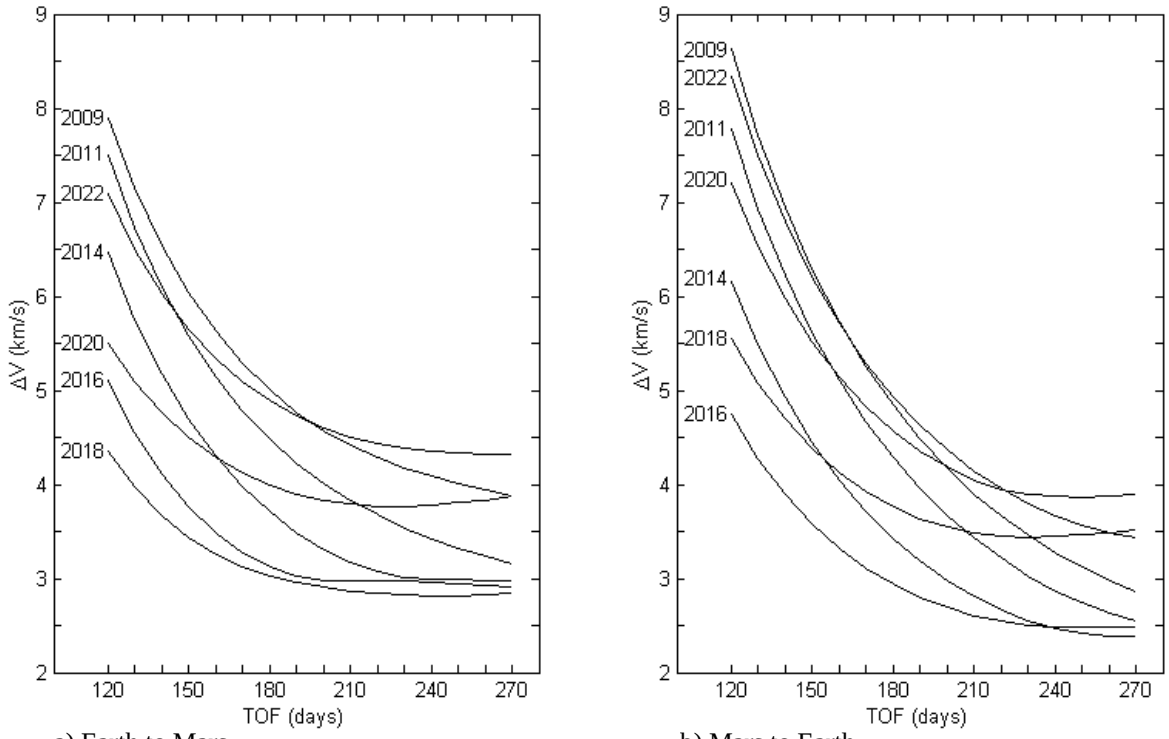

a) Earth to Mars b) Mars to Earth

Fig. 13 ΔV for low-thrust transfers with aerocapture or direct entry.

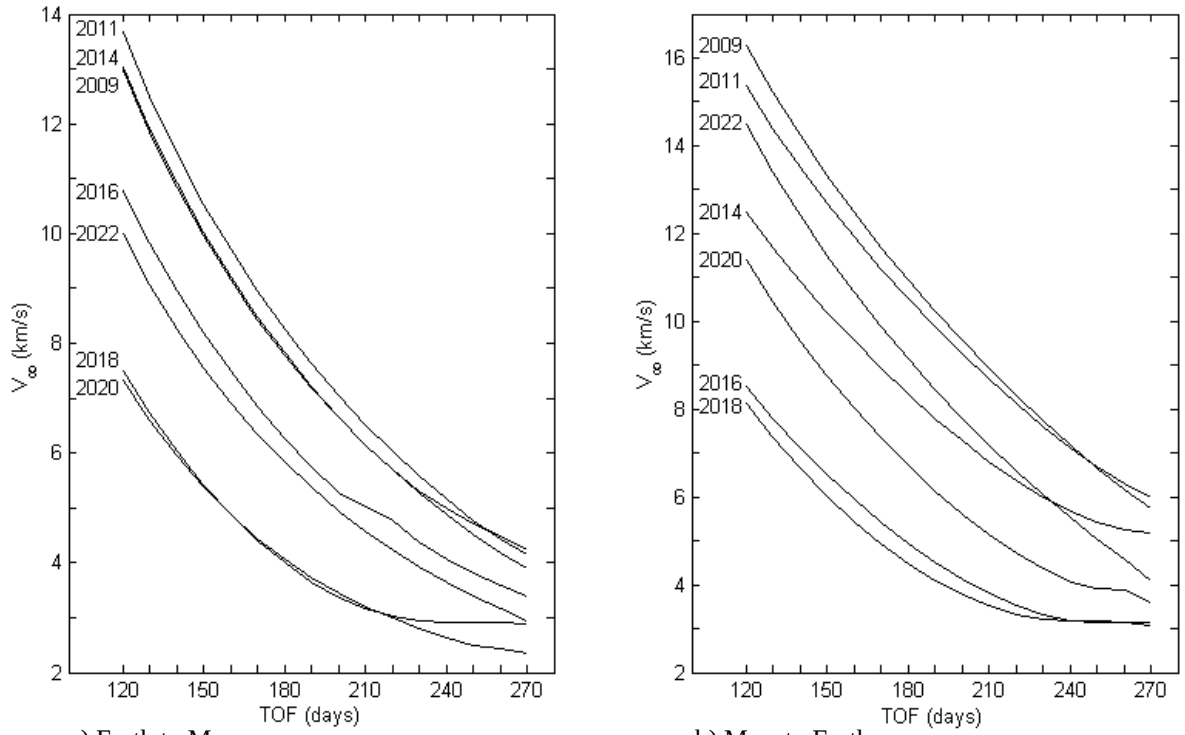

a) Earth to Mars b) Mars to Earth

Fig. 14 Arrival V_∞ for low-thrust transfers with aerocapture or direct entry.

A notable difference between the impulsive-ΔV curves and the minimum-thrust curves (Fig. 12) is that the impulsive transfers typically flatten out by 270-day TOF (i.e. a local minimum exists below a TOF of 270 days) whereas the minimum-thrust ΔV continue to decrease at 270-day TOF. The aero-assisted low-thrust curves (Fig. 13) do not exhibit the same behavior because the thrust was set to a specific value (determined from Fig. 12) for each launch year and TOF combination. Indeed, there is a range of optimal ΔV values for a given launch opportunity and maximum TOF as the thrust varies from a minimum value to infinity (i.e. impulsive thrusting). The trajectories in Fig. 12–Fig. 14 are designed to limit the thrust requirements of an electric propulsion system to the lowest practical values for the crew transfer vehicles. (Certainly, lower thrust and longer TOF would be appropriate for cargo transfers.)

Further, the low-thrust curves do not rise as sharply as the impulsive-ΔV curves at low TOF. In Fig. 12 the ΔV doubles from 270- to 150-day TOF (similar to most impulsive transfers), but the 120-day TOF ΔV is only about 2.6 times the 270-day TOF ΔV across each launch opportunity (the corresponding impulsive-ΔV ratio is significantly higher). The relative ΔV reduction from 180-day TOF to 270-day TOF for minimum-thrust trajectories is about 40%, while the relative reduction from 180 days to 210 days is closer to 17% across all launch opportunities. The aero-assisted capture trajectories increase at a less uniform rate over the different launch opportunities. For example, the ΔV ratio from a TOF of 270 days to 120 days is only about 1.5 when Mars is near perihelion (during 2016–2018), but the same ratio is approximately 2.4 (for Earth-Mars transfers) and 3.0 (for Mars-Earth transfers) when Mars is at aphelion (during 2009–2011). The impulsive aero-assisted direct trajectories exhibit a relatively steeper rise from 270- to 120-day TOF, yet retain the same disparity between trajectories when Mars is at perihelion or aphelion. There is also a broad range in the reduction in ΔV from 180-day TOF to 270-day TOF aero-assisted trajectories. When Mars in near perihelion the reduction is only about 5% (for the given thrust levels), but the ΔV is reduced by up to 30% for outbound transfers and 40% for the inbound trajectories when Mars is near aphelion. The mass savings that may be gained by extending the allowable TOF depends mainly on the vehicle mass and I_{sp}, but a TOF extension of only one or two months can lead to a considerable reduction in mission mass.

V. Conclusions

To further explore the available options for human missions to Mars, we have calculated the minimum-ΔV direct, free-return, Mars-Earth semi-cycler, Earth-Mars semi-cycler, and cycler trajectories with the stipulation that each trajectory must provide a short TOF transfer (from 120 to 270 days) from Earth to Mars and back. All seven launch opportunities during the 2009–2022 synodic-period cycle were included in our analysis. The 2009 and 2022 launch opportunities (when Mars is near aphelion) require the most ΔV, while the 2016 and 2018 launch years (when Mars is near perihelion) often provide the lowest ΔV transfers. Among the five trajectory types, the rank order in terms of V_∞ and ΔV requirements (from lowest to highest) is direct, free-return, Earth-Mars semi-cycler, Mars-Earth semi-cycler, then cycler. Because the ΔV for free-return trajectories are usually similar to the direct trajectory ΔV, this additional safety feature may be incorporated into Mars missions at relatively little cost. In the free-return case, the total mission time is similar to the direct trajectory mission time, but in the event of abort the crew must remain in space for up to three years. We also find that aero-assisted trajectories require significantly lower departure V_∞ and higher arrival V_∞ when compared to powered capture trajectories. A practical feature of low-thrust trajectories for Mars missions is that the optimal ΔV is relatively independent of the vehicle parameters for a given TOF and burn time. This property leads to a simple method for computing the minimum thrust necessary to travel between Earth and Mars as a function of TOF, vehicle mass, and I_{sp}.

Though the most efficient way to guard a crew from the hazards of radiation and zero-gravity during a Mars mission is still unresolved, additional crew protection such as artificial gravity or radiation shielding could replace propellant mass (through the reduction of ΔV) by extending the TOF beyond six months. For example, at the expense of one month of additional TOF (to 210 days), the ΔV is reduced by 10%–20% on average or up to about 2 km/s of ΔV, while a three-month extension to 270 days results in an average savings of 15%–45% with up to 4 km/s of ΔV eliminated from the mission. Similar trades in TOF may be performed among the various Earth-Mars trajectory options, which have been compiled for the first time with respect to a maximum allowable TOF. The optimal trajectory characteristics (Fig. 6–Fig. 35) are particularly useful for preliminary design studies of human missions to Mars.

Appendix

The following figures (Fig. 15–Fig. 35) provide the optimal total ΔV, the DSM ΔV, the Mars stay time, the total mission duration, and the arrival and departure V_∞ at Earth and Mars as functions of maximum TOF for each of the seven launch opportunities between 2009 and 2022. We note that an increase in ΔV for semi-cyclers and cyclers during one launch year is always balanced by a reduction in ΔV during other launch years; in this way the total ΔV for a sustained Mars program is minimized. The mean of the ΔV, the mean of the stay time and mission duration, and the root-mean square of the V_∞ of the trajectory data for a given TOF over the seven missions is used to compute the values in Fig. 6, Fig. 7, and Fig. 8, respectively. Similarly, the maximum of each trajectory parameter during the seven synodic periods is given in Fig. 9–Fig. 11. The data in the appendix follow a 15-year cycle, thus the 2009 data provides a good estimate for missions launched in 2024.

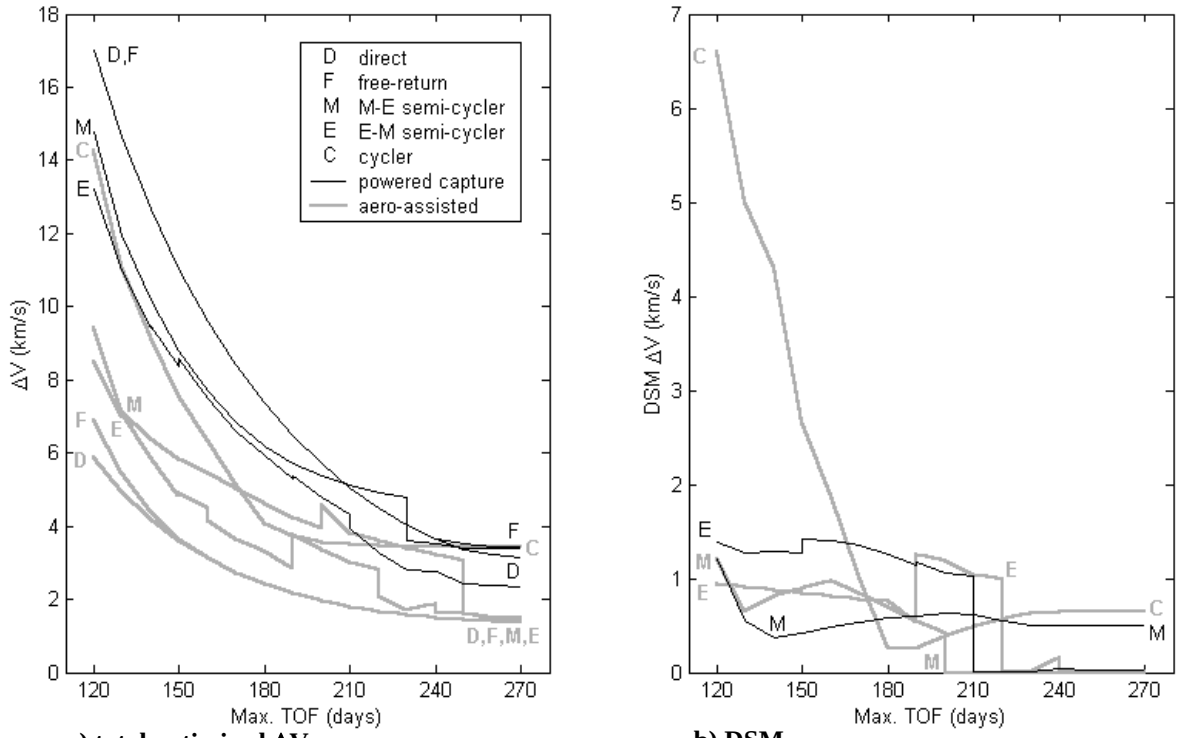

a) total optimized ΔV **b) DSM**

Fig. 15 Δ*V* during 2009 launch opportunity.

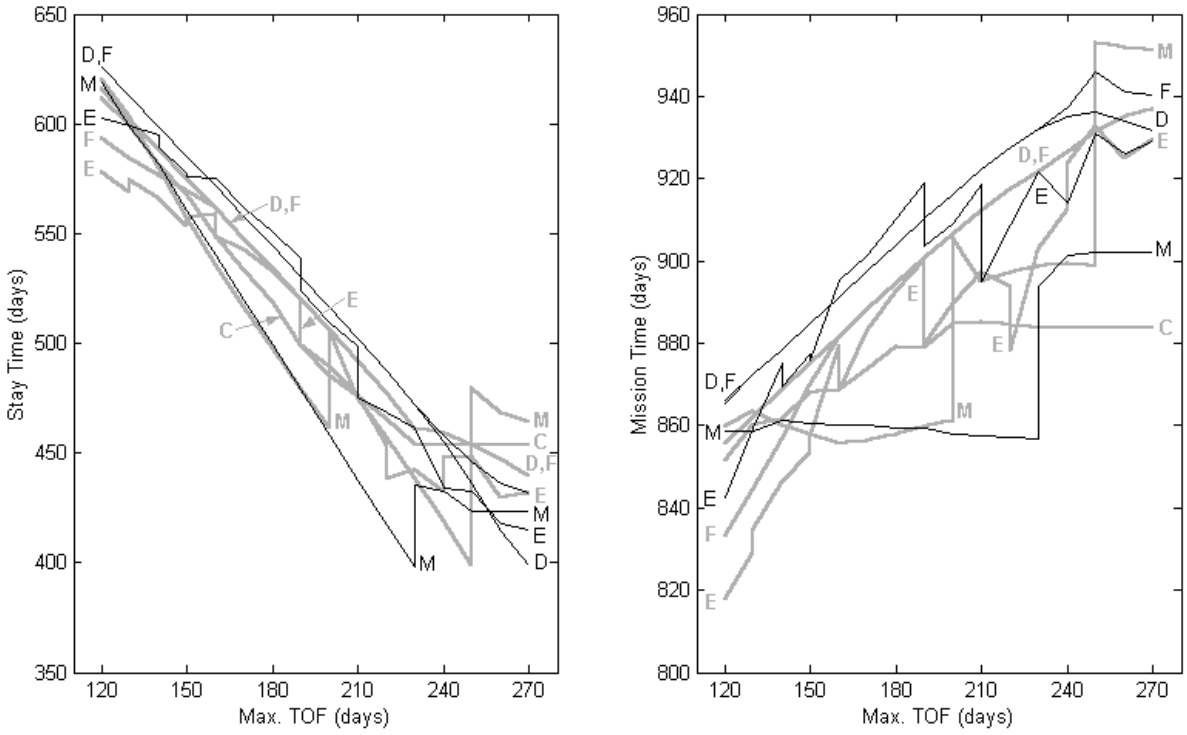

a) Mars stay time **b) total mission duration**

Fig. 16 Stay time and mission time during 2009 launch opportunity.

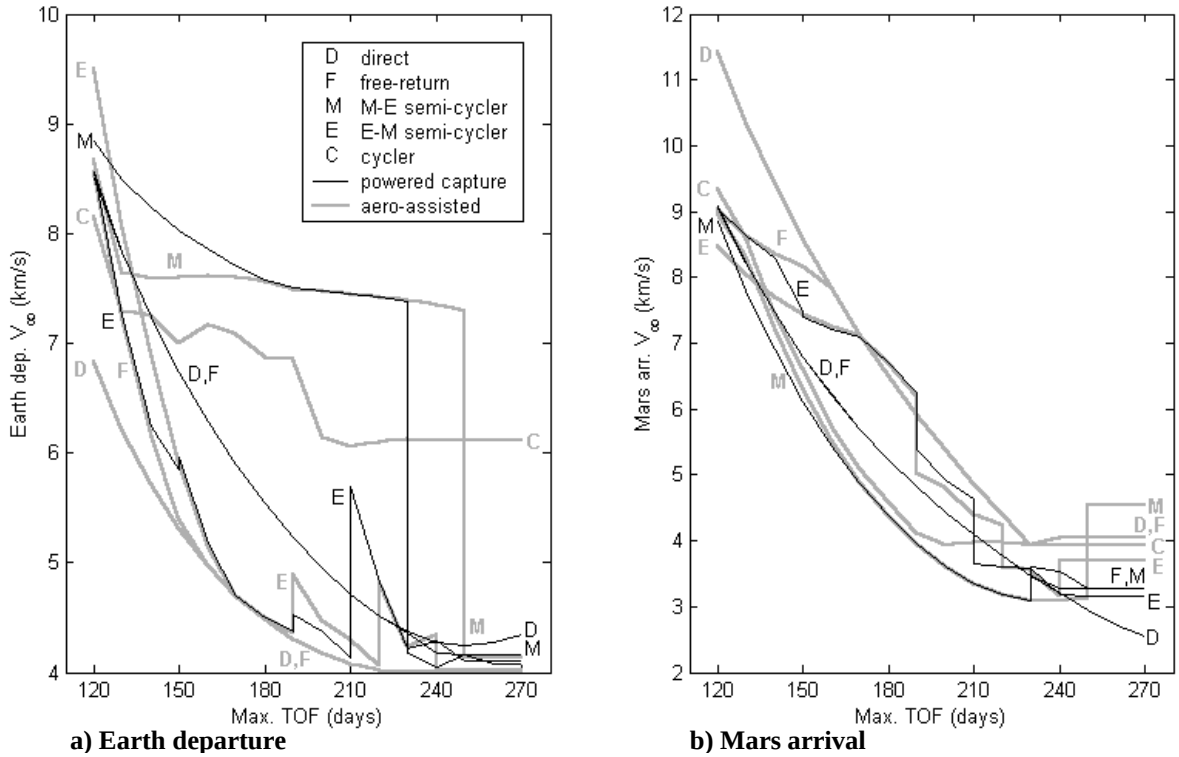

a) Earth departure

b) Mars arrival

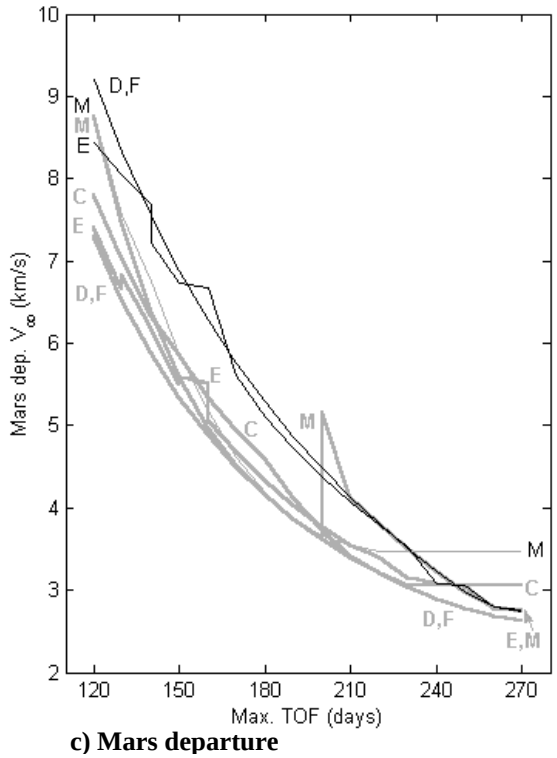

c) Mars departure

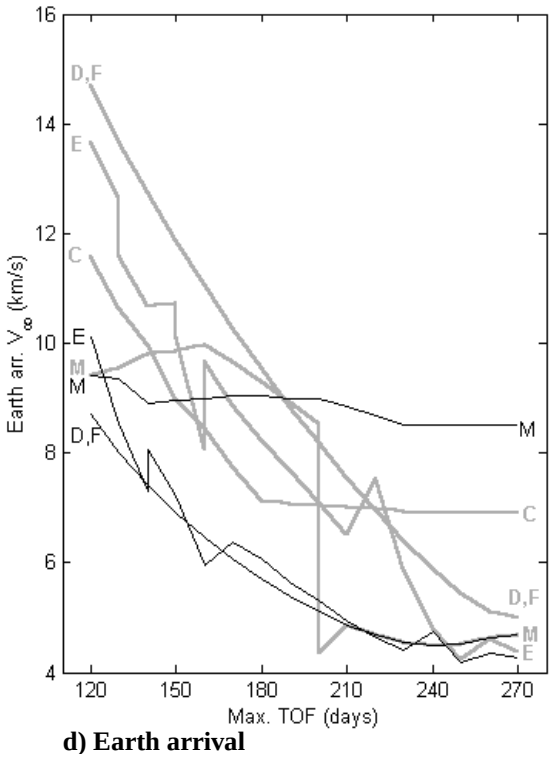

d) Earth arrival

Fig. 17 V_∞ during 2009 launch opportunity.

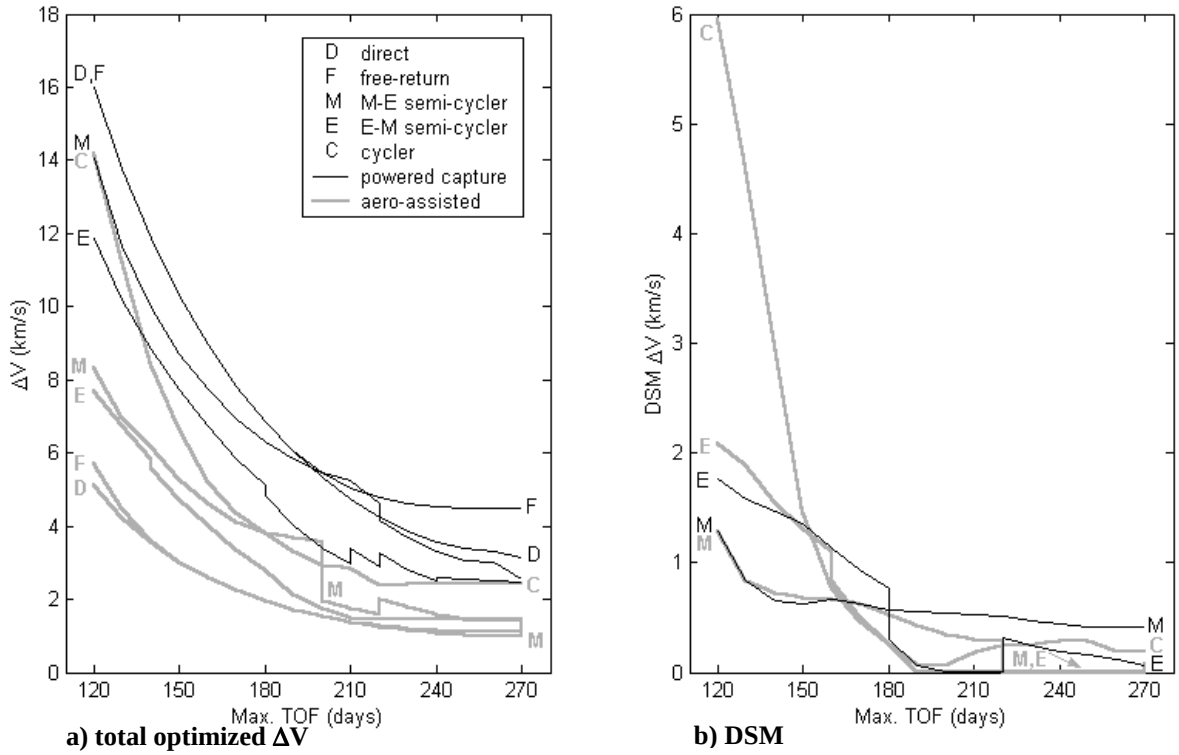

a) total optimized ΔV **b) DSM**

Fig. 18 Δ*V* during 2011 launch opportunity.

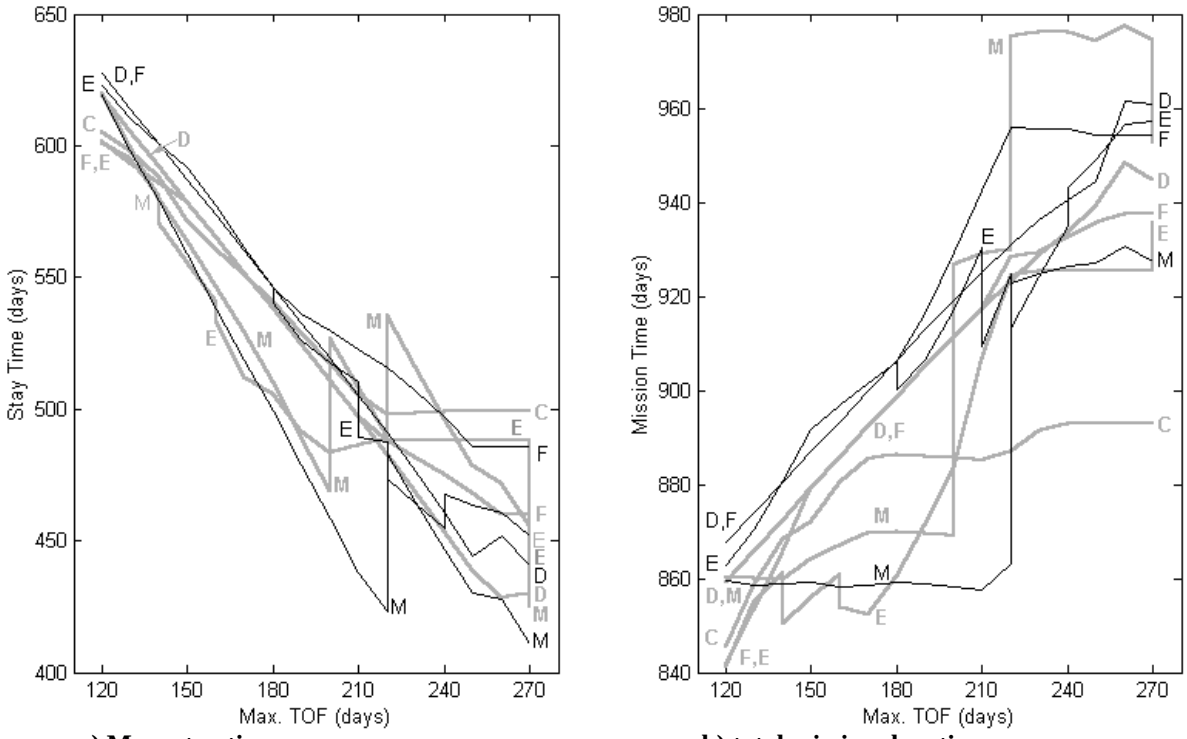

a) Mars stay time **b) total mission duration**

Fig. 19 Stay time and mission time during 2011 launch opportunity.

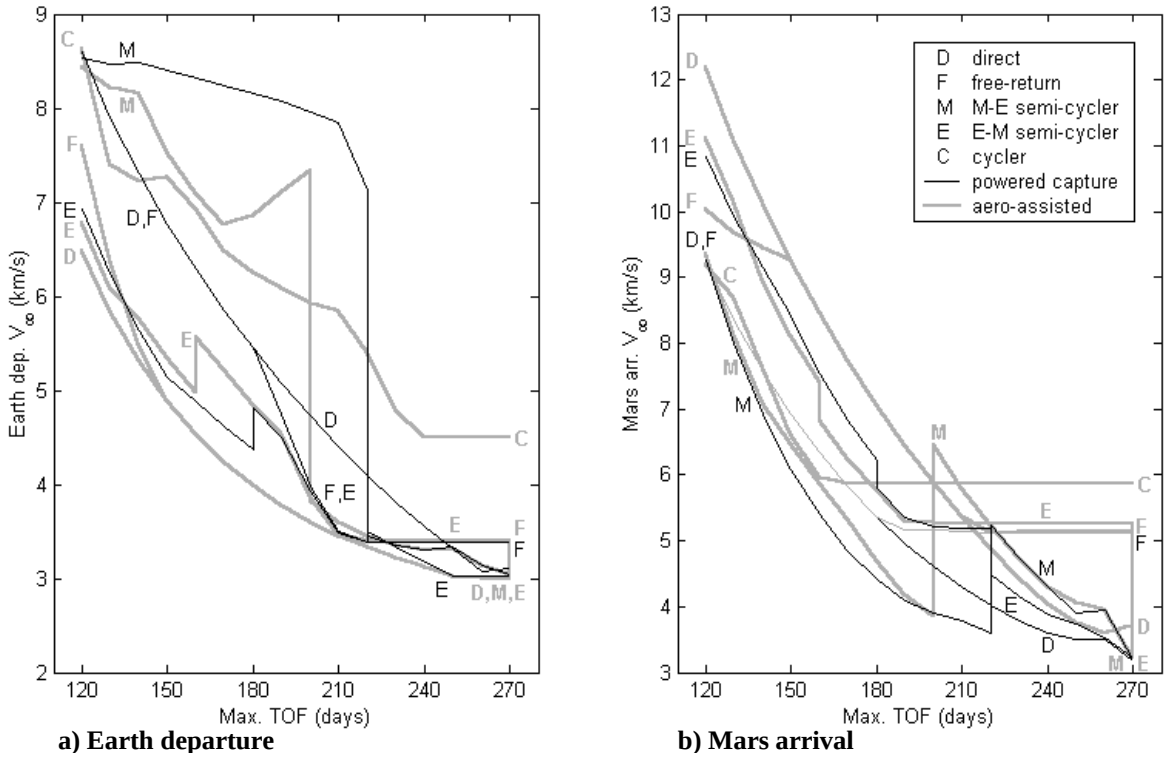

a) Earth departure **b) Mars arrival**

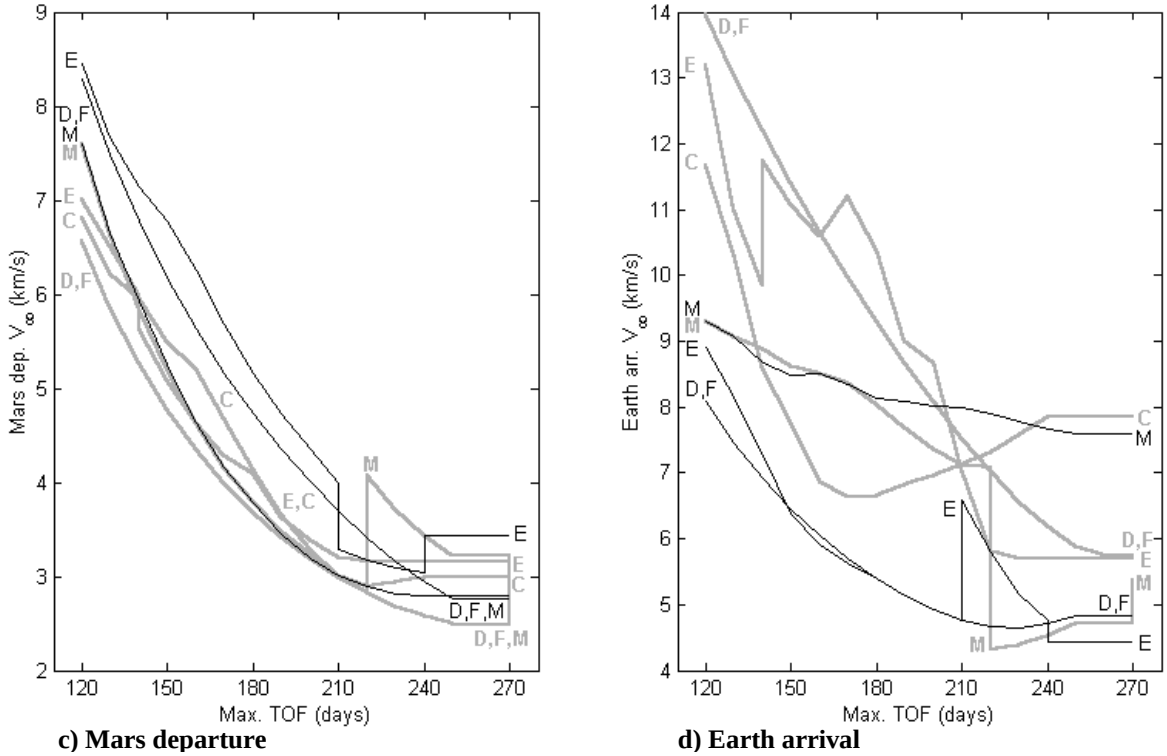

c) Mars departure **d) Earth arrival**

Fig. 20 V_∞ during 2011 launch opportunity.

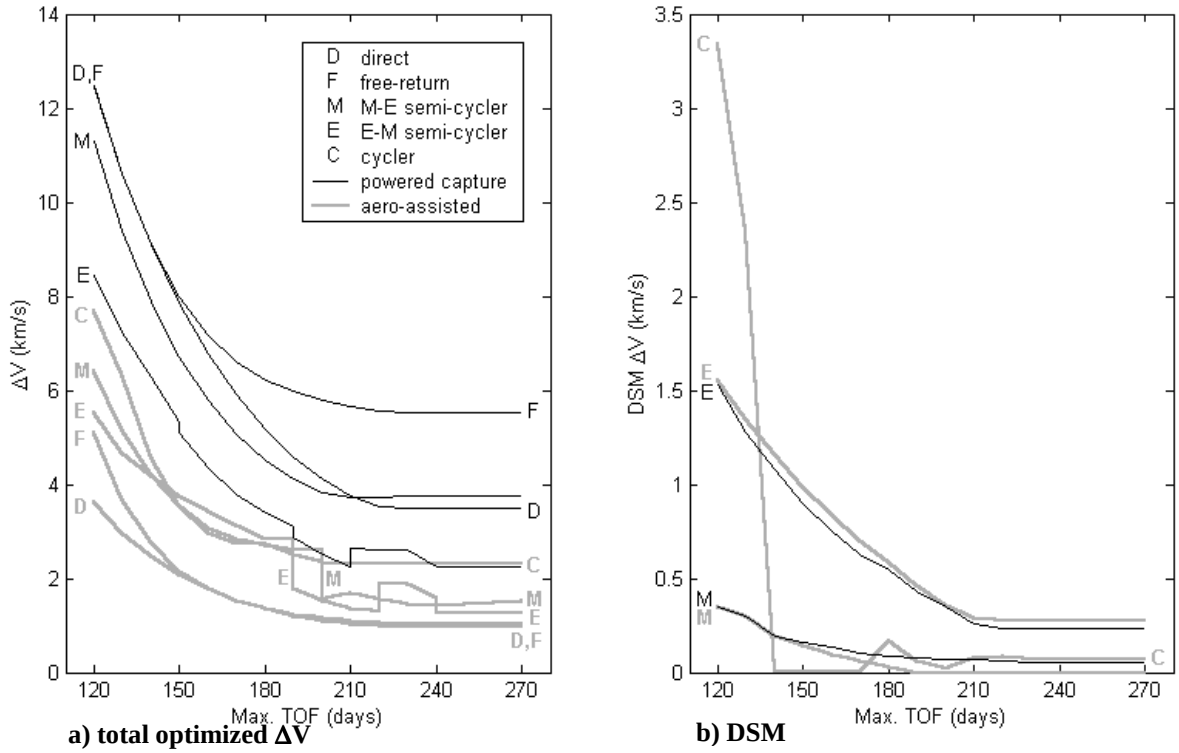

a) total optimized ΔV **b) DSM**

Fig. 21 Δ*V* during 2014 launch opportunity.

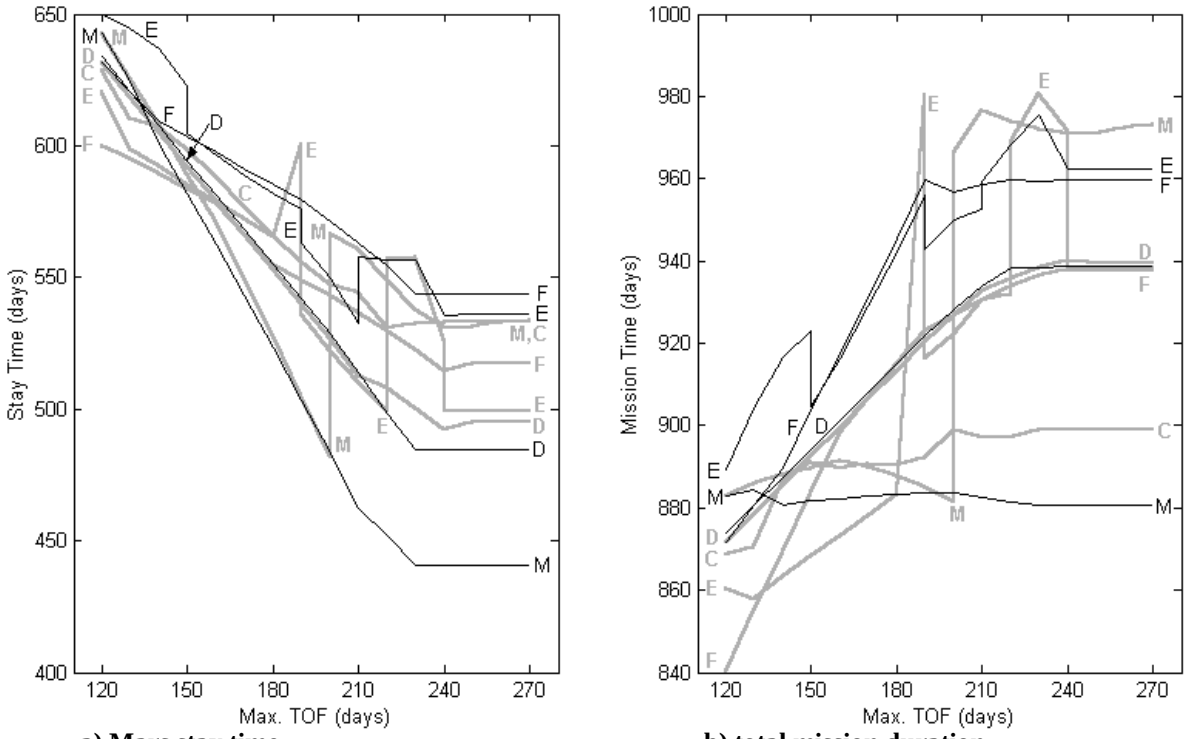

a) Mars stay time **b) total mission duration**

Fig. 22 Stay time and mission time during 2014 launch opportunity.

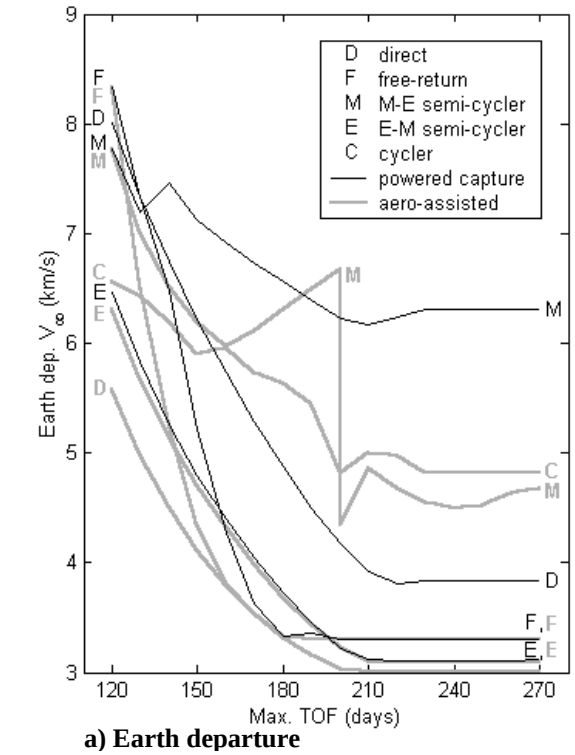

a) Earth departure

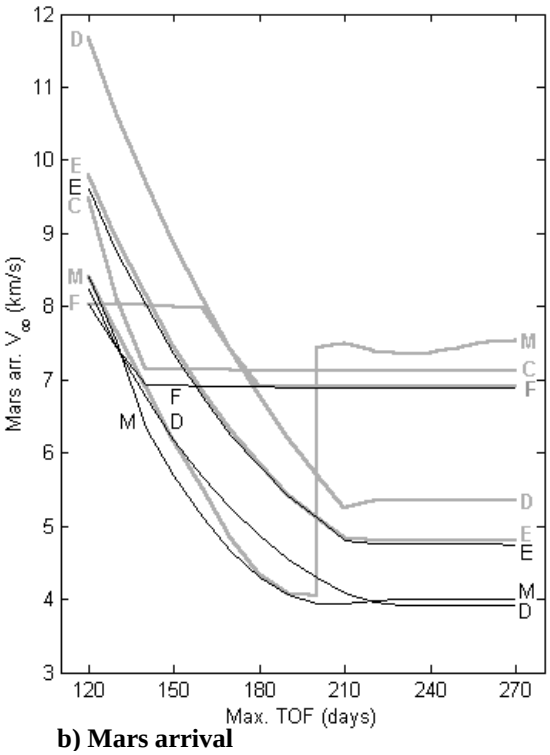

b) Mars arrival

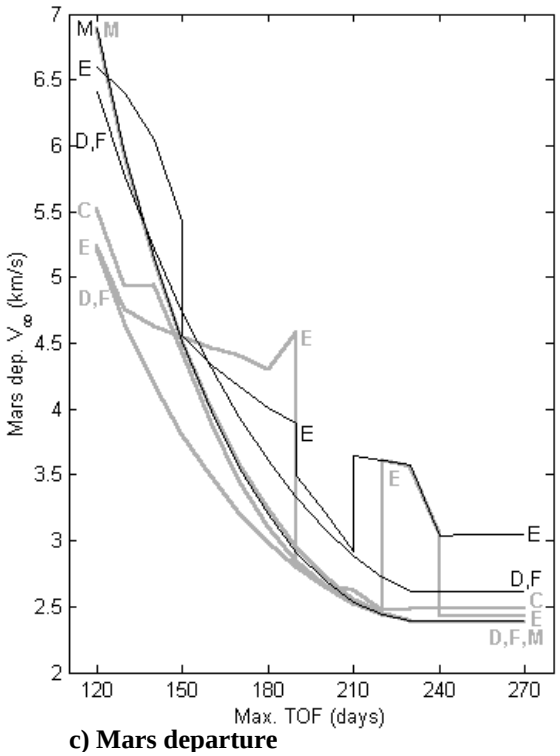

c) Mars departure

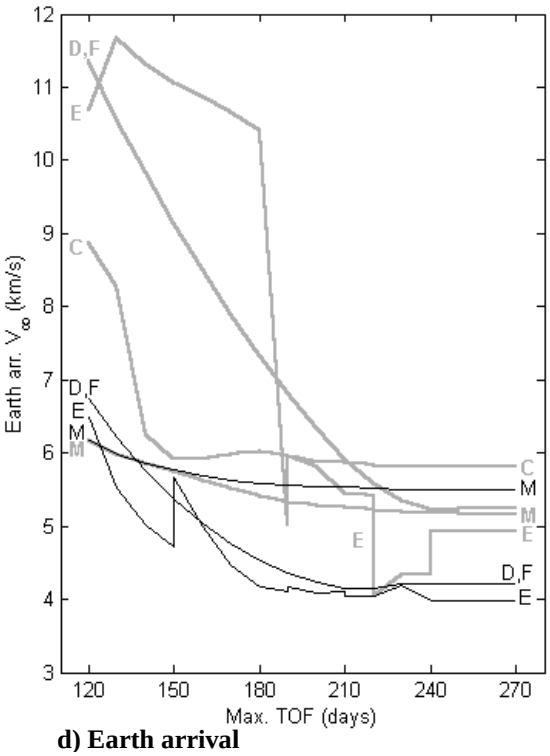

d) Earth arrival

Fig. 23 V∞ during 2014 launch opportunity.

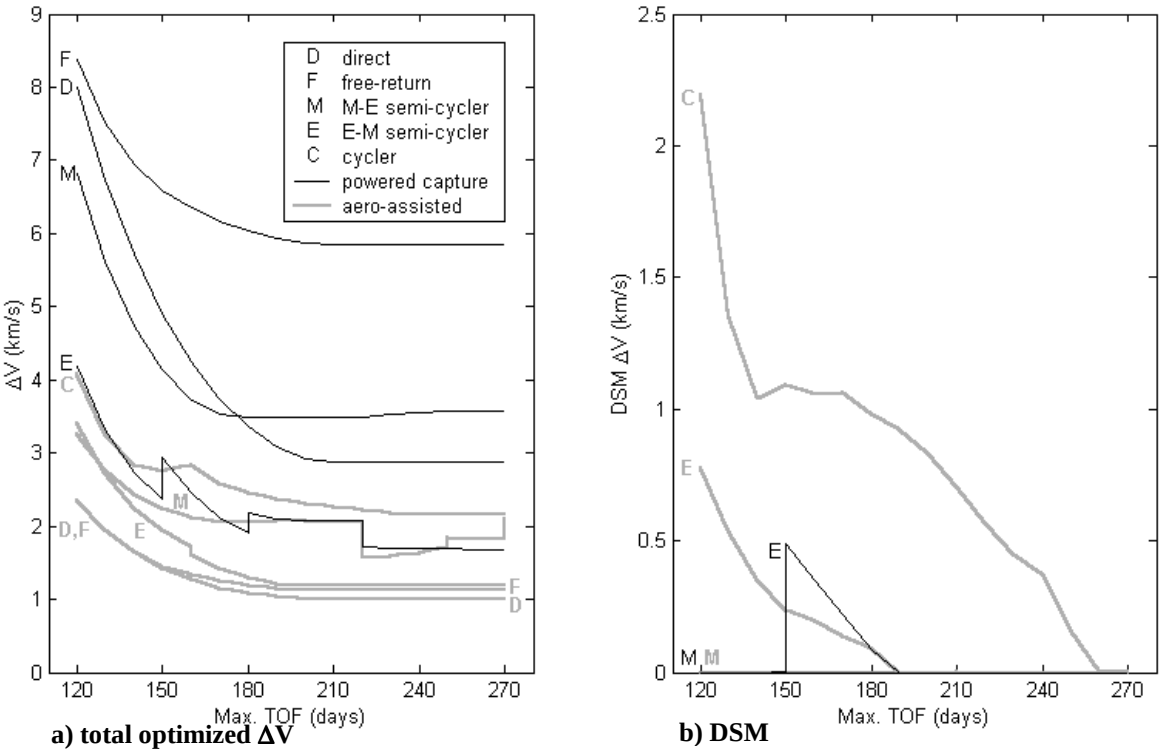

a) total optimized ΔV **b) DSM**

Fig. 24 Δ*V* during 2016 launch opportunity.

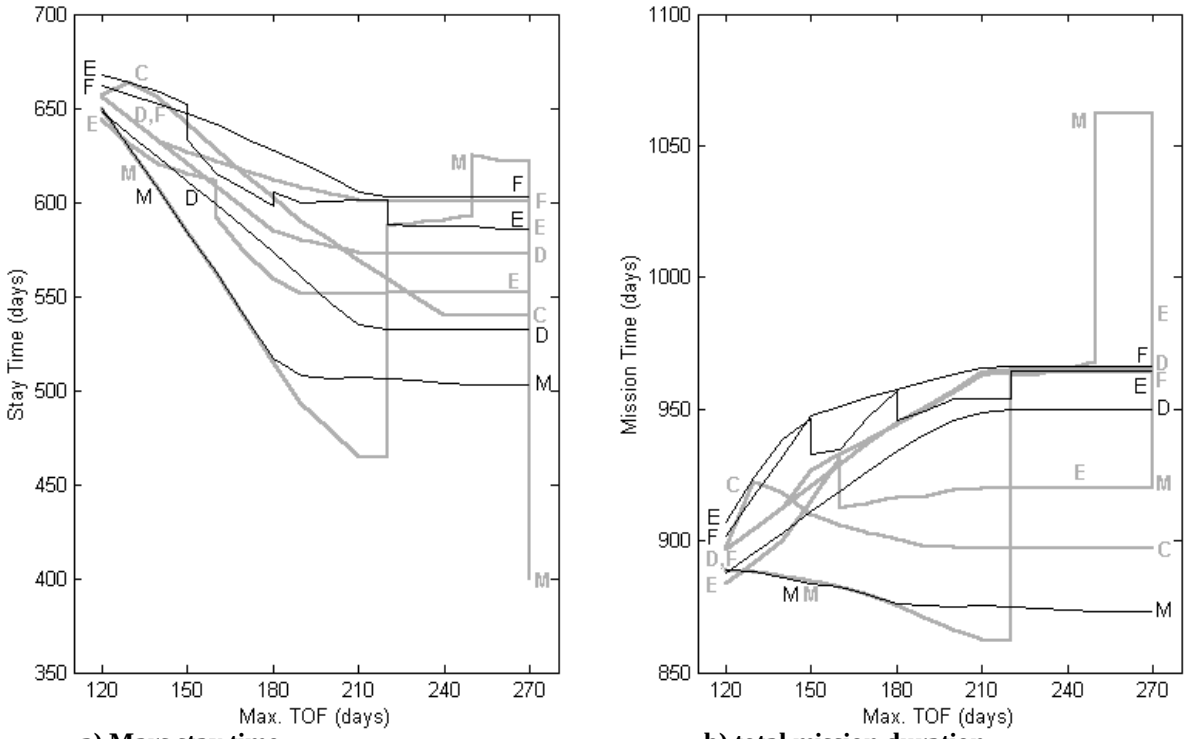

a) Mars stay time **b) total mission duration**

Fig. 25 Stay time and mission time during 2016 launch opportunity.

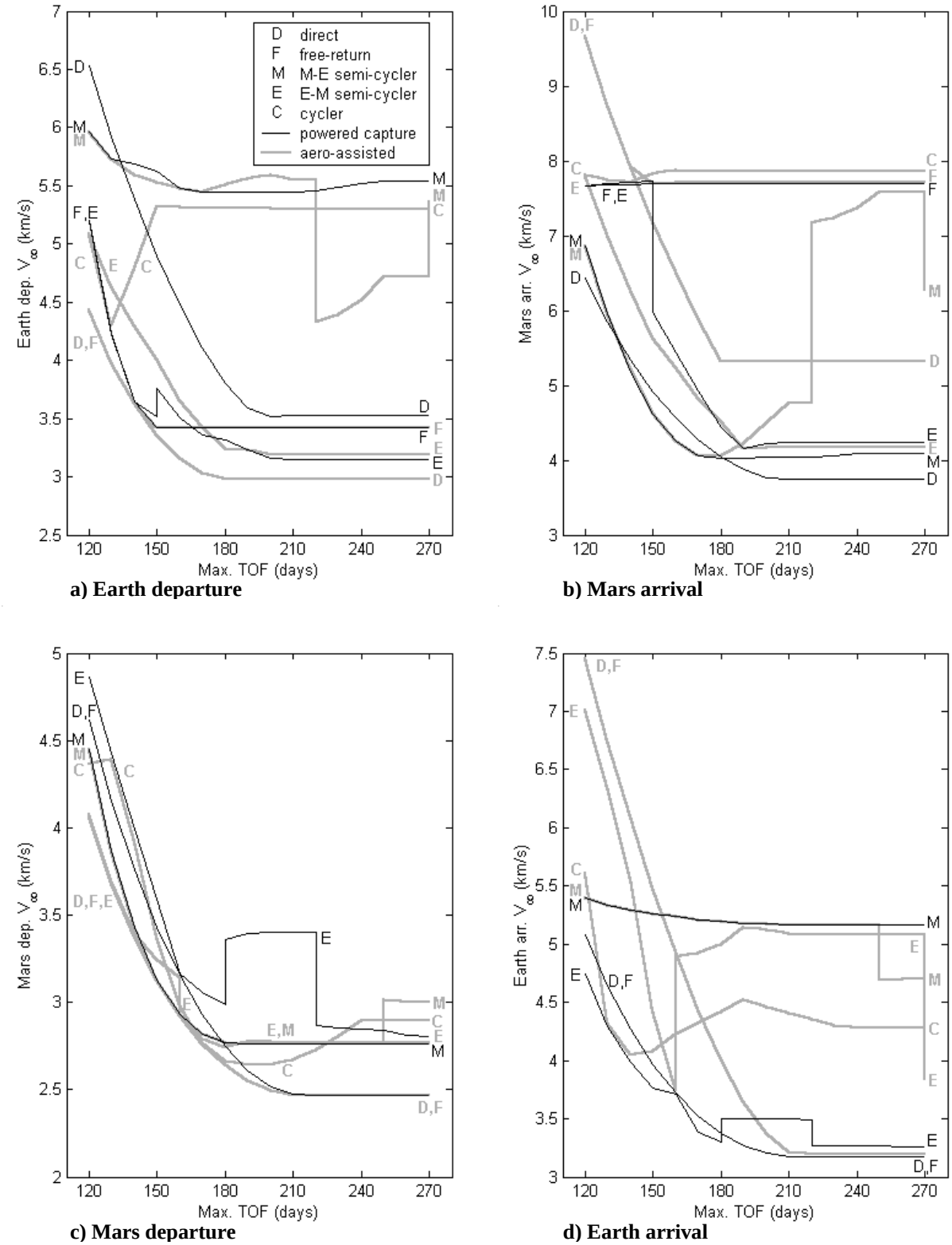

a) Earth departure **b) Mars arrival**

c) Mars departure **d) Earth arrival**

Fig. 26 V_∞ during 2016 launch opportunity.

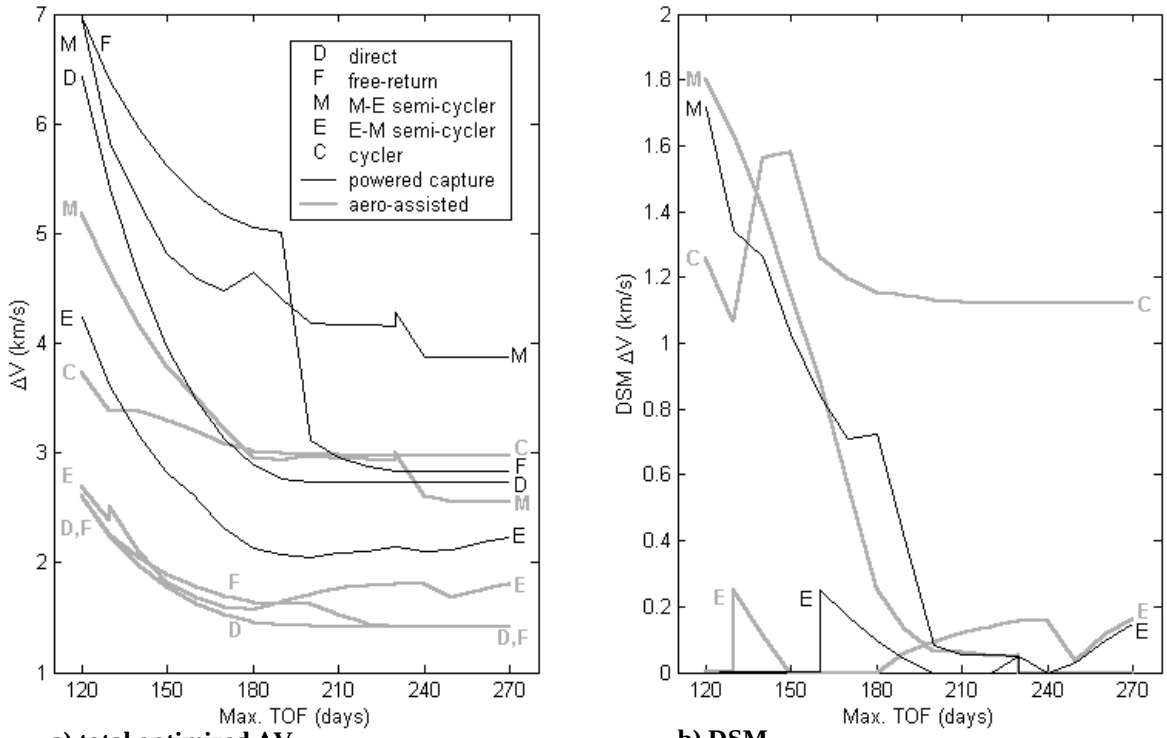

a) total optimized ΔV **b) DSM**

Fig. 27 Δ*V* during 2018 launch opportunity.

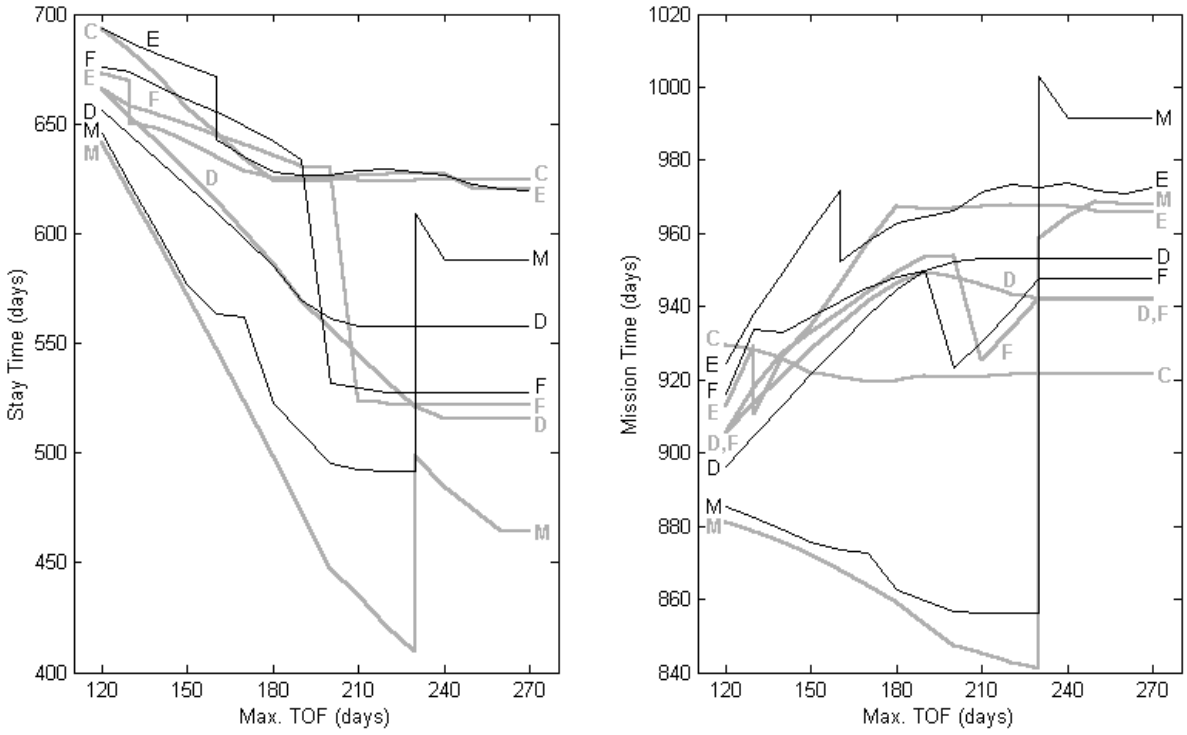

a) Mars stay time **b) total mission duration**

Fig. 28 Stay time and mission time during 2018 launch opportunity.

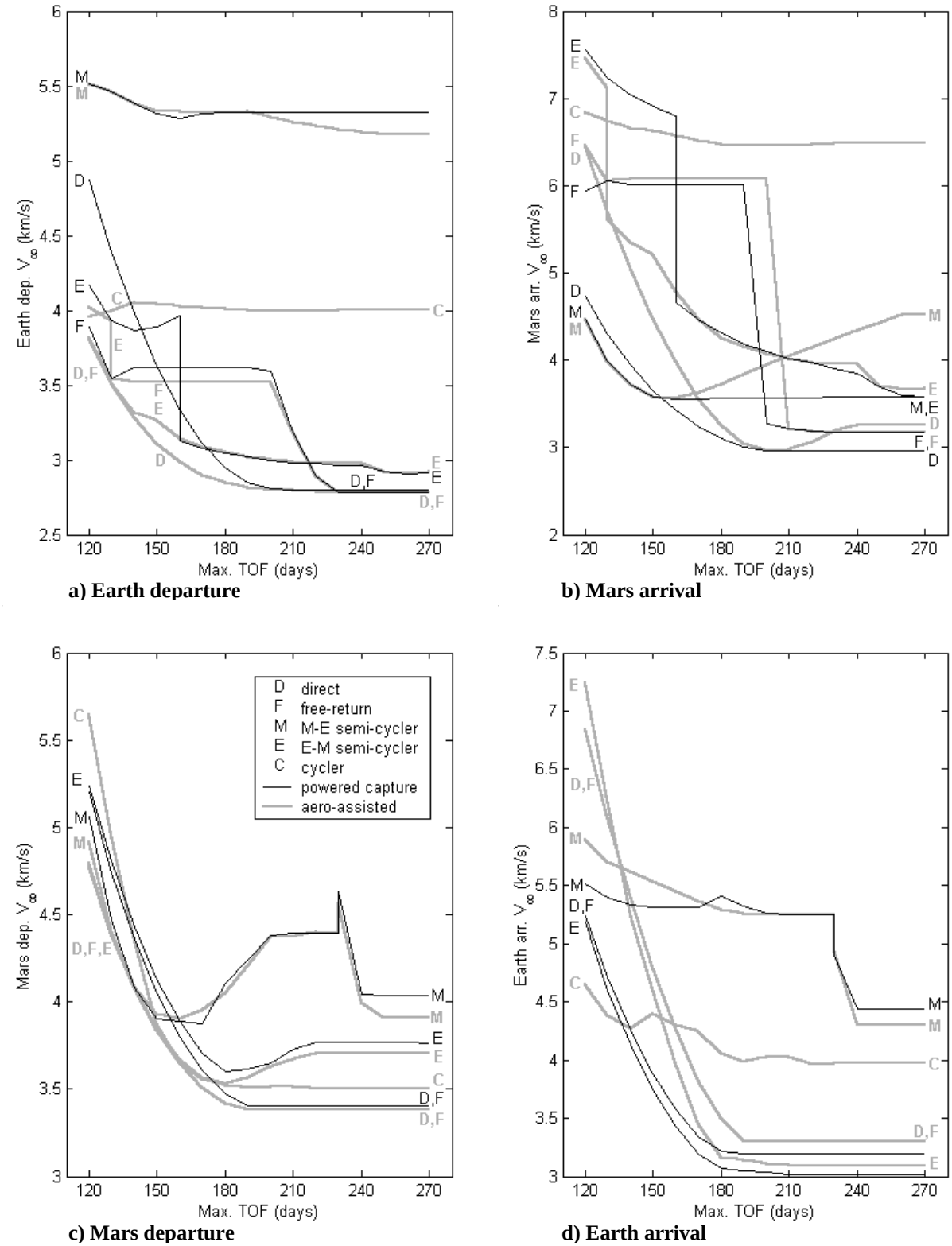

a) Earth departure **b) Mars arrival**

c) Mars departure **d) Earth arrival**

Fig. 29 V_∞ during 2018 launch opportunity.

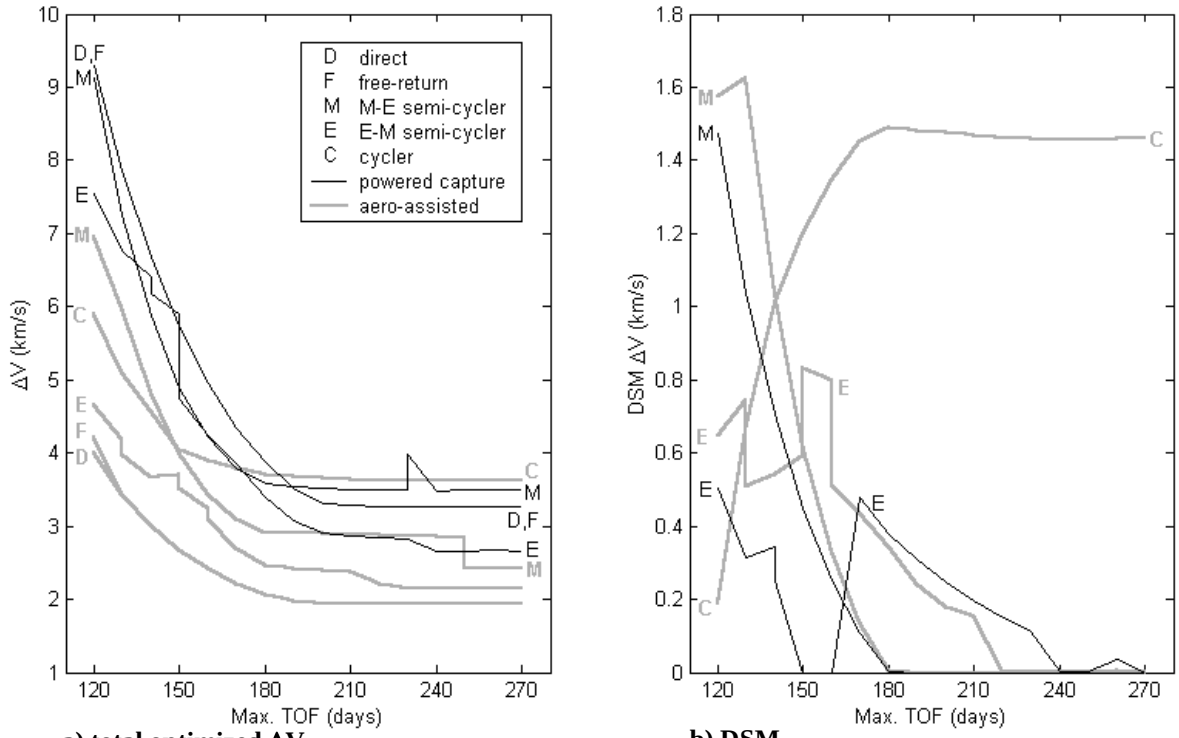

a) total optimized ΔV **b) DSM**

Fig. 30 Δ*V* during 2020 launch opportunity.

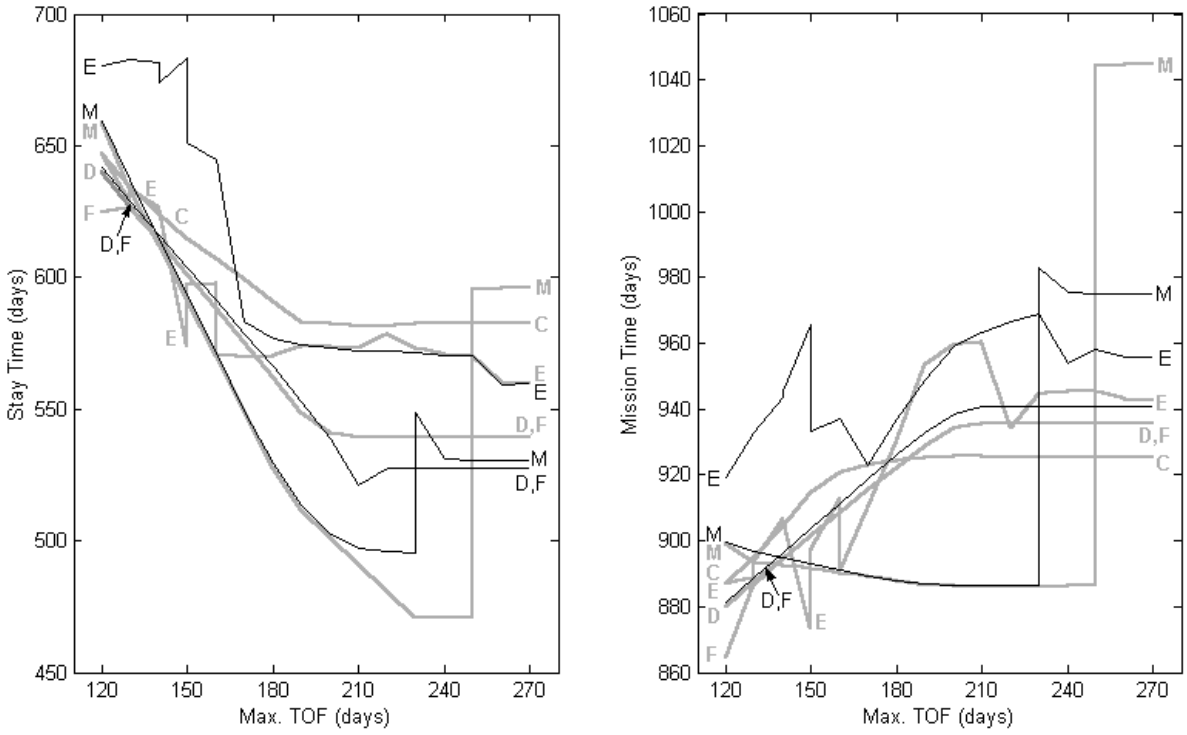

a) Mars stay time **b) total mission duration**

Fig. 31 Stay time and mission time during 2020 launch opportunity.

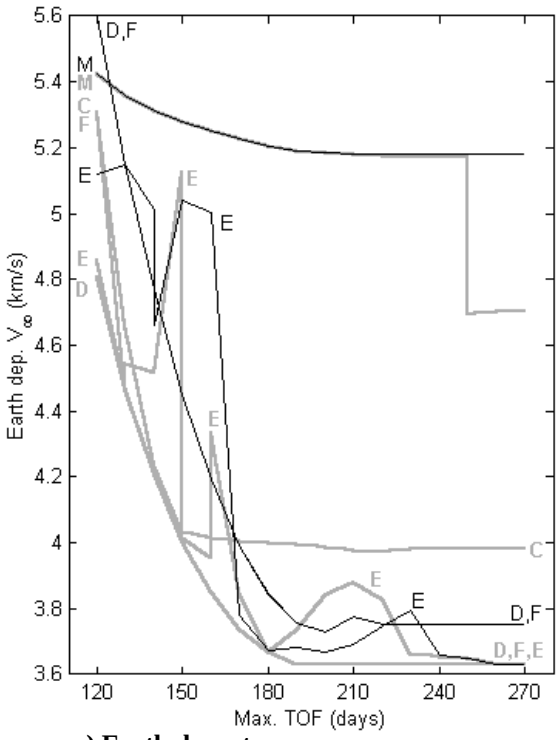

a) Earth departure

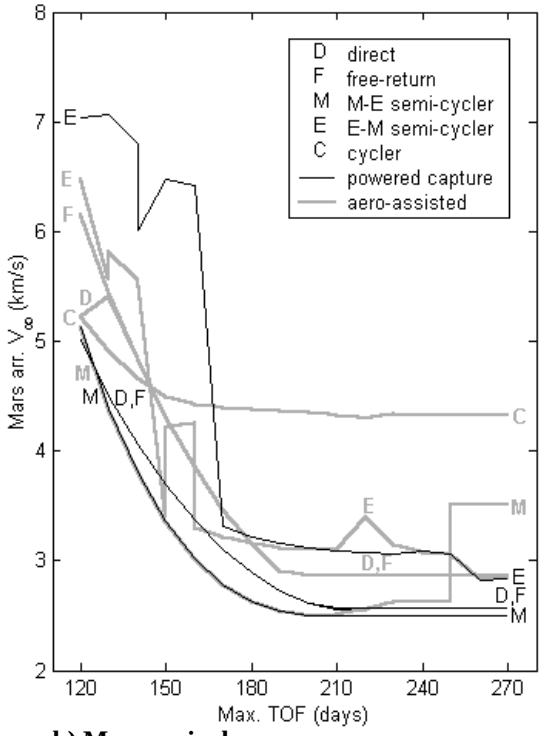

b) Mars arrival

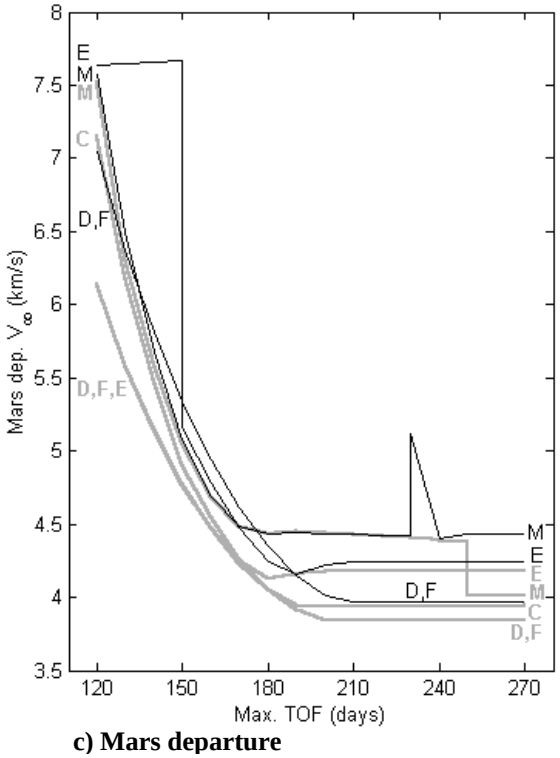

c) Mars departure

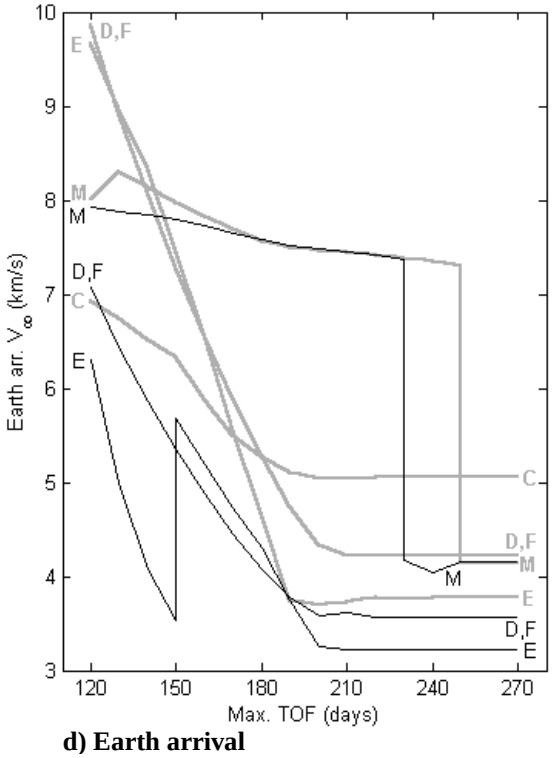

d) Earth arrival

Fig. 32 V_∞ during 2020 launch opportunity.

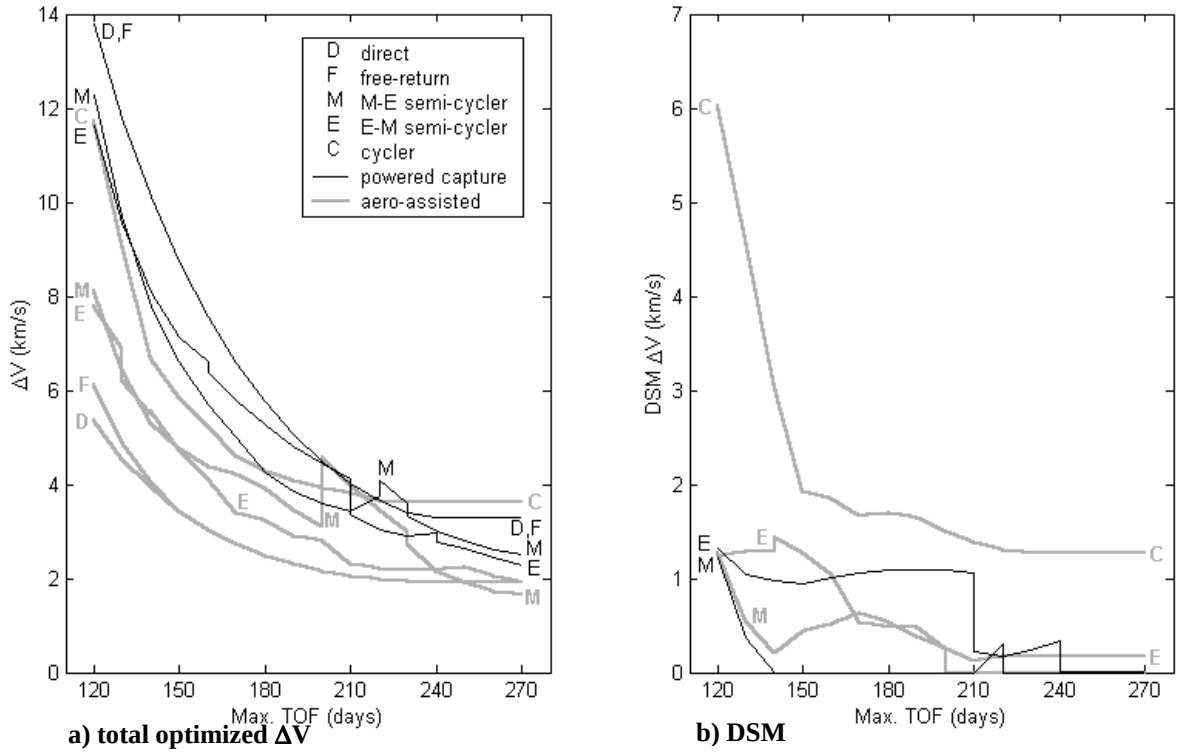

a) total optimized ΔV **b) DSM**

Fig. 33 Δ*V* during 2022 launch opportunity.

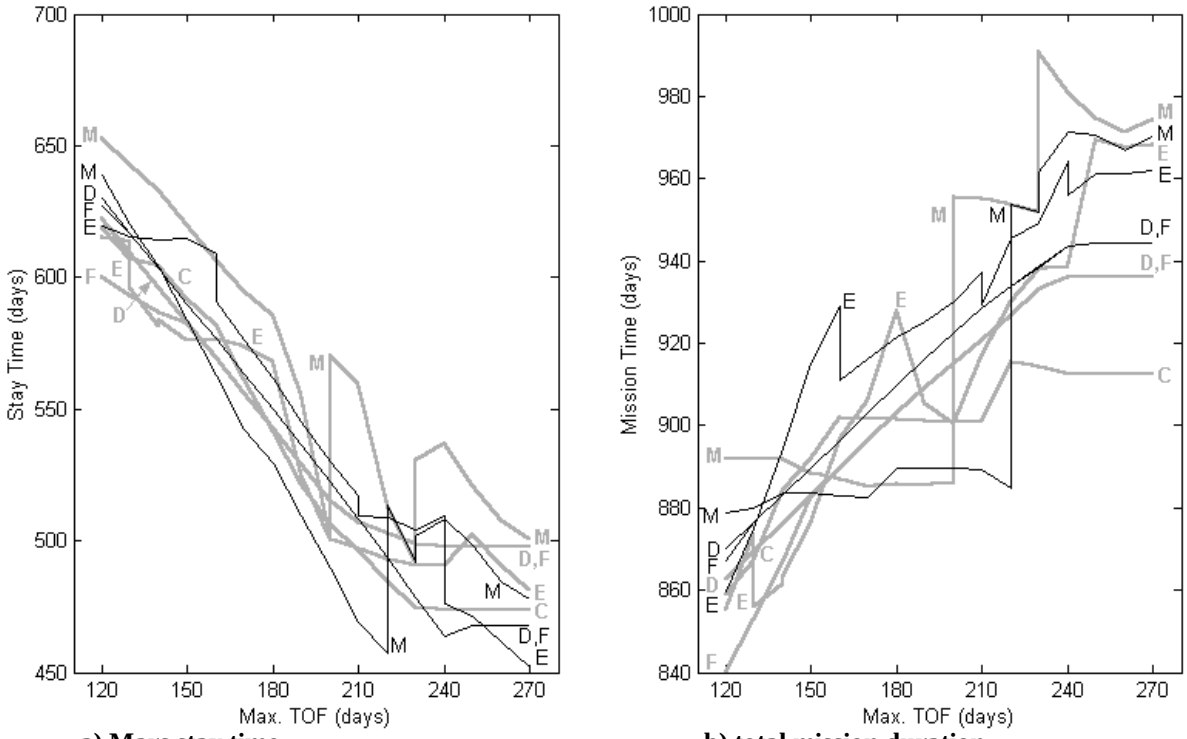

a) Mars stay time **b) total mission duration**

Fig. 34 Stay time and mission time during 2022 launch opportunity.

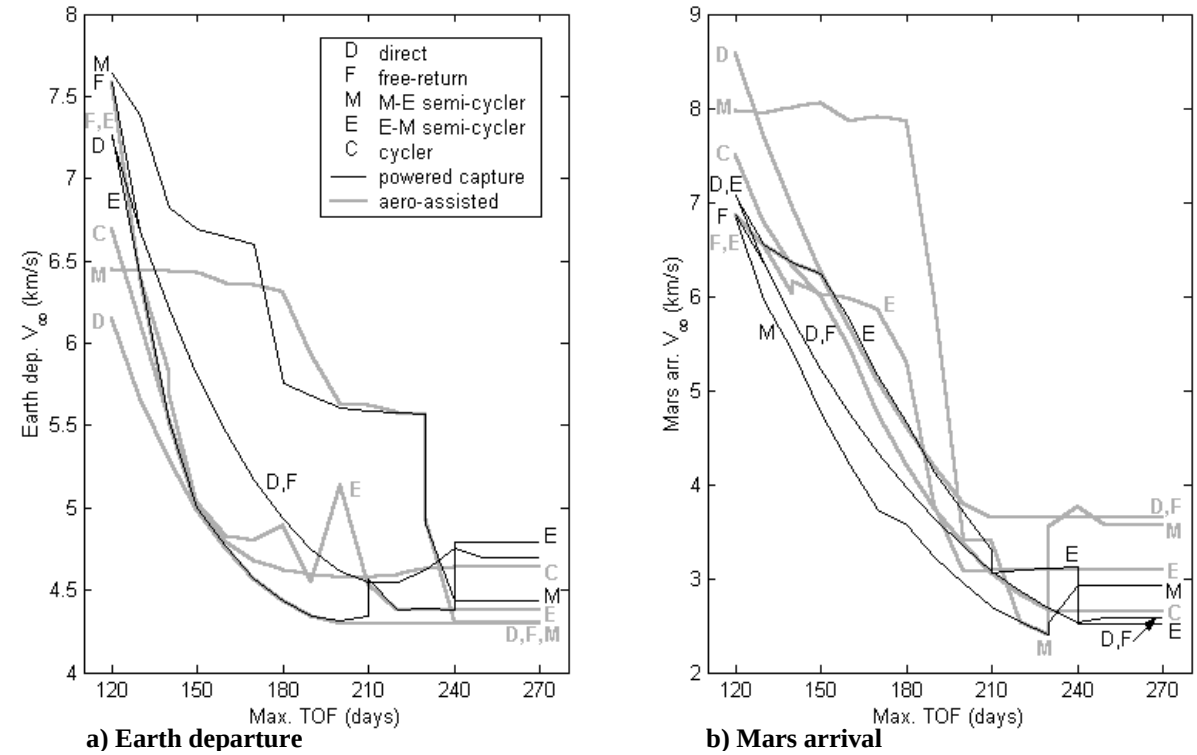

a) Earth departure **b) Mars arrival**

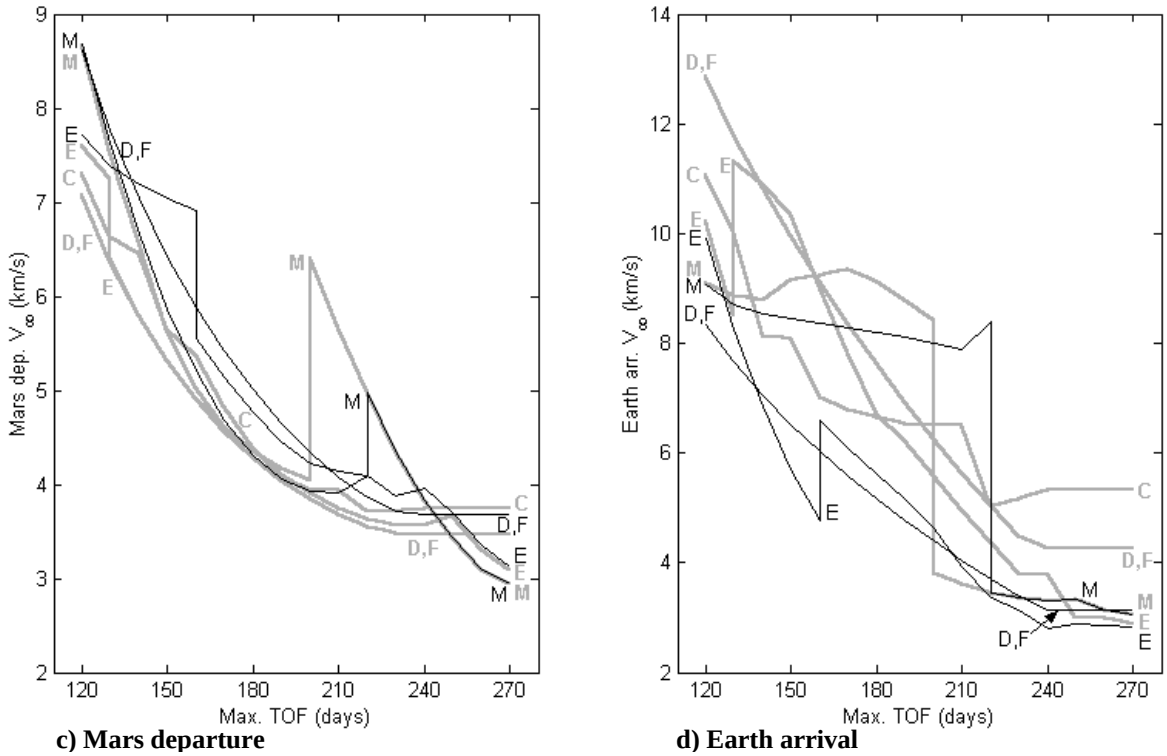

c) Mars departure **d) Earth arrival**

Fig. 35 V_∞ during 2022 launch opportunity.

Acknowledgments

The first author's work has been sponsored in part by a National Defense Science and Engineering Graduate (NDSEG) Fellowship.

References

[1]Von Braun, W., *The Mars Project*, University of Illinois Press, Urbana, IL, 1953.

[2]Ehricke, K. A., Whitlock, C. M., Chapman, R. L., and Purdy, C. H., "Calculations on a Manned Nuclear Propelled Space Vehicle," ARS Report 532-57, 1957.

[3]Irving, J. H. and Blum, E. K., "Comparative Performance of Ballistic and Low-Thrust Vehicle for Flight to Mars," *Vistas in Astronautics*, Vol. II, Pergamon Press, 1959, pp.191-218.

[4]Himmel, S. C., Dugan, J. F., Luidens, R. W., and Weber, R. J., "A Study of Manned Nuclear-Rocket Missions to Mars," Aerospace Engineering, Vol. 20, July 1961, pp. 18, 19, 51-58.

[5]Gillespie, R. W., Ragsac, R. V., Ross, S. E., "Prospects for Early Manned Interplanetary Flights," *Astronautics and Aerospace Engineering*, Vol. 1, August 1963, pp. 16-21.

[6]Von Braun, W., "The Next 20 Years of Interplanetary Exploration," *Astronautics and Aeronautics*, Vol. 3, November 1965, pp. 24-34.

[7]Hoffman, S. J., Friedlander, A. L., and Nock, K. T., "Transportation Mode Performance Comparison for a Sustained Manned Mars Base," AIAA Paper 86-2016, AIAA/AAS Astrodynamics Conference, Williamsburg, VA, Aug. 18-20, 1986.

[8]Cohen, A., *The 90 Day Study on the Human Exploration of the Moon and Mars*, U.S. Government Printing Office, Washington, DC, 1989.

[9]Braun, R. D. and Blersch, D. J., "Propulsive Options for a Manned Mars Transportation System," *Journal of Spacecraft and Rockets*, Vol. 28, No. 1, 1993, pp. 85-92.

[10]Walberg, G., "How Shall We Go to Mars? A Review of Mission Scenarios," *Journal of Spacecraft and Rockets*, Vol. 30, No. 2, 1993, pp. 129-139.

[11]Niehoff, J. C. and Hoffman, S. J., "Pathways to Mars: An Overview of Flight Profiles and Staging Options for Mars Missions," AAS Paper 95-478, *Science and Technology Series of the American Astronautical Society*, Vol. 86, San Diego, CA, Univelt, Inc., 1996, pp. 99-125.

[12]Zubrin, R., *The Case for Mars*, Simon and Schuster, Inc., New York, NY, 1996.

[13]Hoffman, S. and Kaplan, D., eds., "Human Exploration of Mars: The Reference Mission of the NASA Mars Exploration Study Team," NASA SP 6107, 1997.

[14]Drake, B. G., ed., "Reference Mission Version 3.0 Addendum to the Human Exploration of Mars: The Reference Mission of the NASA Mars Exploration Study Team," Exploration Office Document EX 13-98-036, June 1998,
see also http://ares.jsc.nasa.gov/HumanExplore/Exploration/EXLibrary/docs/MarsRef/addendum/index.htm.

[15]Donahue, B. B. and Cupples, M. L., "Comparative Analysis of Current NASA Human Mars Mission Architectures," *Journal of Spacecraft and Rockets*, Vol. 38, No. 5, 2001, pp.745-751.

[16]Landau, D. F. and Longuski, J. M., "Comparative Assessment of Human Missions to Mars," AAS Paper 03-513, AAS/AIAA Astrodynamics Specialist Conference, Big Sky, MT, August 4-7, 2003.

[17]Sohn, R. L., "Venus Swingby Mode for Manned Mars Missions," *Journal of Spacecraft and Rockets* Vol. 1, No. 5, 1964, pp. 565-567.

[18]Titus, R. R., "FLEM–Flyby-Landing Excursion Mode," AIAA Paper 66-36, Aerospace Sciences Meeting, New York, NY, July 26-29, 1965.

[19]Deerwester, J. M. and Dhaem, S. M., "Systematic Comparison of Venus Swingby Mode with Standard Mode of Mars Round Trips," *Journal of Spacecraft and Rockets* Vol. 4, July 1967, pp. 904-911.

[20]Gillespie, R. W. and Ross, S., "Venus-Swingby Mode and Its Role in the Manned Exploration of Mars," *Journal of Spacecraft and Rockets* Vol. 4, February 1967, pp. 170-175.

[21]Casalino, L., Colasurdo, G., Pastrone, D., "Optimization Procedure for Preliminary Design of Opposition-Class Mars Missions," *Journal of Guidance, Control, and Dynamics*, Vol. 21, No. 1, 1998, pp. 134-140.

[22]Breakwell, J. V., Gillespie, R. W., and Ross, S. E., "Researches in Interplanetary Flight," *ARS Journal*, Vol. 31, No. 2, 1961, pp.201-207.

[23]Knip, G. and Zola, C. L., "Three-Dimensional Trajectory Analysis for Round-Trip Mission to Mars," NASA TN-D-1316, 1962.

[24]Ross, S., "Planetary Flight Handbook," NASA SP-35, 1963.

[25]Lee, V. A. and Wilson, S. W., "A Survey of Ballistic Mars-Mission Profiles," *Journal of Spacecraft and Rockets*, Vol. 4, No. 2, 1967, pp. 129-142.

[26]Young, A. C., Mulqueen, J. A., and Skinner, J. E., "Mars Exploration, Venus Swingby and Conjunction Class Mission Modes, Time Period 2000-2045," NASA TM-86477, 1984.

[27]Gravier, J. P., Marchal, C., Culp, R. D., "Optimal Trajectories Between Earth and Mars in Their True Planetary Orbits," *Journal of Optimization Theory and Applications*, Vol. 9, February 1972, pp. 120-136.
[28]Hoffman, S. J., McAdams, J. V., and Niehoff, J. C., "Round Trip Trajectories for Human Exploration of Mars," AAS Paper 89-201, 1989.
[29]Soldner, J. K., "Round Trip Mars Trajectories: New Variations on Classic Mission Profiles," AIAA Paper 90-2932, August 1990.
[30]George, L. E. and Kos, L. D., "Interplanetary Mission Design Handbook: Earth-to Mars Mission Opportunities and Mars-to-Earth Return Opportunities 2009-2024," NASA TM-1998-208533, 1998.
[31]Munk, M. M., "Departure Energies, Trip Times, and Entry Speeds for Human Mars Missions," American Astronautical Society, AAS Paper 99-103, 1999.
[32]Miele, A. and Wang, T., "Optimal Transfers from an Earth Orbit to a Mars Orbit," *Acta Astronautica*, Vol. 45, No. 3, 1999, pp. 119-133.
[33]Penzo, P. and Nock, K., "Earth-Mars Transportation Using Stop-Over Cyclers," AIAA Paper 2002-4424, AIAA/AAS Astrodynamics Specialist Conference, Monterey, CA, August 2-5 2002.
[34]Crocco, G. A., "One Year Exploration Trip Earth-Mars-Venus-Earth," *Proceedings of the 10th International Astronautical Federation*, Rome, 1956.
[35]Battin, R. H, "The Determination of Round-Trip Planetary Reconnaissance Trajectories," *Journal of Aerospace Sciences*, Vol. 26, No. 9, 1959, pp. 545-567.
[36]Ruppe, H. O., "Interplanetary Flight," *Handbook of Astronautical Engineering*, H. H. Koelle, ed., McGraw-Hill Book Company, New York, 9.32-9.44, 1961.
[37]Hénon, M., "Interplanetary Orbits which Encounter the Earth Twice," *Bulletin Astronomique*, Vol. 3, No. 3, 1968, pp.377-393.
[38]Wolf, A., A., "Free Return Trajectories for Mars Missions," AAS Paper 91-123, AAS/AIAA Spaceflight Mechanics Meeting, San Diego, CA, February 11-13, 1991.
[39]Patel, M. R., Longuski, J. M., and Sims, J. A., "Mars Free Return Trajectories," *Journal of Spacecraft and Rockets* Vol. 35, No. 3, 1998, pp. 350-354.
[40]Miele, A., Wang, T., and Mancuso, S., "Optimal Free-Return Trajectories for Moon Missions and Mars Missions," *Journal of the Astronautical Sciences*, Vol. 48, Nos. 2-3, 2000, pp.183-206.
[41]Okutsu, M. and Longuski, J. M., "Mars Free-Returns via Gravity Assist from Venus," *Journal of Spacecraft and Rockets* Vol. 39, No. 1, 2002, pp. 31-36.
[42]Bishop, R. H., Byrnes, D. V., Newman, D. J., Carr, C. E., and Aldrin, B., "Earth-Mars Transportation Opportunities: Promising Options for Interplanetary Transportation," American Astronautical Society, AAS Paper 00-255, The Richard H. Battin Astrodynamics Conference, College Station, TX, March 20-21, 2000.
[43]Aldrin, B., Byrnes, D., Jones, R., and Davis, H., "Evolutionary Space Transportation Plan for Mars Cycling Concepts," AIAA Paper 2001-4677, Albuquerque, NM, August 2001.
[44]Hollister, W. M, "Castles in Space," *Astronautica Acta*, Vol. 14, No. 2, 1969, pp. 311-316.
[45]Rall, C. S. and Hollister, W. M., "Free-Fall Periodic Orbits Connecting Earth and Mars," AIAA Paper 71-92, 1971.
[46]Byrnes, D. V., Longuski, J. M., and Aldrin, B., "Cycler Orbit Between Earth and Mars," *Journal of Spacecraft and Rockets*, Vol. 30, No. 3, May-June 1993, pp. 334-336.
[47]Byrnes, D. V., McConaghy, T. T, and Longuski, J. M., "Analysis of Various Two Synodic Period Earth-Mars Cycler Trajectories," AIAA Paper 2002-4423, AIAA/AAS Astrodynamics Specialist Conference, Monterey, CA, August 5-8, 2002.
[48]Chen, K. J., McConaghy, T. T., Landau, D. F., and Longuski, J. M., "A Powered Earth-Mars Cycler with Three Synodic-Period Repeat Time," AAS Paper 03-510, AAS/AIAA Astrodynamics Specialist Conference, Big Sky, MT, August 4-7, 2003.
[49]McConaghy, T. T., Yam, C. H., Landau, D. F., and Longuski, J. M., "Two-Synodic-Period Earth-Mars Cyclers with Intermediate Earth Encounter," AAS Paper 03-509, AAS/AIAA Astrodynamics Specialist Conference, Big Sky, MT, August 4-7, 2003.
[50]Moekel, W. E., "Fast Interplanetary Missions with Low-Thrust Propulsion Systems," NASA TR-R-79, 1961.
[51]Melbourne, W. G. and Sauer, C. G., "Optimum Interplanetary Rendezvous with Power-Limited Vehicles," *AIAA Journal*, Vol. 1, No. 1, 1963, pp. 54-60.
[52]Zola, C. L., "A Method for Approximating Propellant Requirements of Low-Thrust Trajectories," NASA TN-D-3400, 1966.
[53]Ragsac, R. V., "Study of Electric Propulsion for Manned Mars Missions," *Journal of Spacecraft and Rockets*, Vol. 4, April 1967, pp. 462-468.
[54]Kawaguchi, J., Takiura, K., and Matsuo, H., "On the Optimization and Application of Electric Propulsion to Mars and Sample and Return Mission," AAS Paper 94-183, AAS/AIAA Spaceflight Mechanics Meeting, Cocoa Beach, FL, February 1994.
[55]Chang-Diaz, F. R., Hsu, M. M., Braden, E., Johnson, I., Yang, T. F., "Rapid Mars Transits with Exhaust Modulated Plasma Propulsion," NASA TP-3539, 1995.
[56]Tang, S. and Conway, B. A., "Optimization of Low-Thrust Interplanetary Trajectories Using Collocation and Nonlinear Programming," *Journal of Guidance, Control, and Dynamics*, Vol. 18, No. 3, 1995, pp. 599-604.
[57]Gefert, L. P., Hack, K. J., and Kerslake, T. W., "Options for the Human Exploration of Mars using Solar Electric Propulsion," STAIF, *Proceedings of the Conferences on Applications of Thermophysics in Microgravity and on Next Generation*

Launch Systems, and 16th Symposium on Space Nuclear Power and Propulsion, Albuquerque, NM, January 31-February 4, 1999, pp. 1275-1280.

[58]Williams, S. N. and Coverstone-Carrol, V., "Mars Missions Using Solar-Electric Propulsion," *Journal of Spacecraft and Rockets*, Vol. 37, No. 1, 2000, pp.71-77.

[59]McConaghy, T. T., Debban, T. J., Petropoulus, A. E., and Longuski, J. M., "An Approach to Design and Optimization of Low-thrust Trajectories with Gravity Assists," AAS Paper 01-468, AAS/AIAA Astrodynamics Specialist Conference, Quebec City, QC, Canada, July-Aug. 2001.

[60]Whiffen, G. J. and Sims, J. A., "Application of the SDC Optimal Control Algorithm to Low-Thrust Escape and Capture Trajectory Optimization," AAS Paper 02-208, AAS/AIAA Space Flight Mechanics Conference, San Antonio, TX, January 27-30, 2002.

[61]Braun, R. D., Powell, R. W., and Hartung, L. C., "Effect of Interplanetary Options on a Manned Mars Aerobrake Configuration," NASA TP-3019, Aug. 1990.

[62]Striepe, S. A., Braun, R. D., Powell, R. W., and Fowler, W. T., "Influence of Interplanetary Trajectory Selection on Earth Atmospheric Velocity of Mars Missions," *Journal of Spacecraft and Rockets*, Vol. 30, No. 4, 1993, pp. 420-425.

[63]Striepe, S. A., Braun, R. D., Powell, R. W., and Fowler, W. T., "Influence of Interplanetary Trajectory Selection on Mars Atmospheric Velocity," *Journal of Spacecraft and Rockets*, Vol. 30, No. 4, 1993, pp. 426-430.

[64]Lyne, J. E., Wercinski, P., Walberg, G., and Jits, R., "Mars Aerocapture Studies for the Design Reference Mission," AAS Paper 98-110, AAS/AIAA Space Flight Mechanics Meeting, Monterey, CA, February 9-11, 1998.

[65]*Optimization Toolbox User's Guide*, The MathWorks, Inc., 2004.

[66]Gill, P. E., Murray, W., and Saunders, M. A., "SNOPT: An SQP Algorithm for Large-Scale Constrained Optimization," *SIAM Journal on Optimization*, Vol. 12, 2002, pp. 979-1006.

[67]D'Amario, L., A., Byrnes, D. V., Sackett, L. L., and Stanford, R. H., "Optimization of Multiple Flyby Trajectories," AAS Paper 79-162, AAS/AIAA Astrodynamics Specialist Conference, Provincetown, MA, June 25-27, 1979.

[68]Sauer, C. G., "Optimization of Interplanetary Trajectories with Unpowered Planetary Swingbys," AAS Paper 87-424, AAS/AIAA Astrodynamics Specialist Conference, Kalispell, MT, August 10-13 1987.

[69]Lawden, D. F., *Optimal Trajectories for Space Navigation*, Butterworths, London 1963.

[70]Jezewski, D.J., "Primer Vector Theory and Applications," NASA TR-R-454, November 1975.

[71]Tsiolkovsky, K. E., "Exploration of the Universe with Reaction Machines," *The Science Review*, #5, St. Petersburg, Russia, 1903.